

New aspects of quantum topological data analysis: Betti number estimation, and testing and tracking of homology and cohomology classes

Junseo Lee* Nhat A. Nghiem†

July 1, 2025

Abstract

The application of quantum computation to topological data analysis (TDA) has received growing attention. While estimating Betti numbers is a central task in TDA, general complexity theoretic limitations restrict the possibility of quantum speedups. To address this, we explore quantum algorithms under a more structured input model. We show that access to additional topological information enables improved quantum algorithms for estimating Betti and persistent Betti numbers. Building on this, we introduce a new approach based on homology tracking, which avoids computing the kernel of combinatorial Laplacians used in prior methods. This yields a framework that remains efficient even when Betti numbers are small, offering substantial and sometimes exponential speedups. Beyond Betti number estimation, we formulate and study the homology property testing problem, and extend our approach to the cohomological setting. We present quantum algorithms for testing triviality and distinguishing homology classes, revealing new avenues for quantum advantage in TDA.

*Team QST, Seoul National University, harris.junseo@gmail.com (Current address: Norma Inc.)

†QuEra Computing Inc. and State University of New York at Stony Brook, nhatanh.nghiemvu@stonybrook.edu

Contents

1	Introduction	3
1.1	Organization of the paper	4
2	Overview and main results	5
2.1	Motivation and problem statement	5
2.2	Input model setup	6
2.3	Estimating Betti numbers	6
2.4	Estimating persistent Betti numbers	9
2.5	Testing for trivial homology classes	10
2.6	Testing homology equivalence	11
2.7	Applications to topological data analysis	13
2.7.1	Tracking homology classes	13
2.7.2	An alternative approach to Betti number estimation	14
2.8	Detecting nontrivial cycles	16
2.9	A cohomology-based algorithm for homology equivalence testing	17
3	Preliminaries and related work	18
3.1	Block-encoding and quantum singular value transformation	18
3.2	Algebraic topology	20
3.3	Topological data analysis	22
4	Alternative quantum algorithm for estimating Betti numbers	25
4.1	Simplicial complex specification	25
4.2	Estimating (normalized) Betti numbers	26
4.3	Estimating (normalized) persistent Betti numbers	28
5	Homology property testing	32
5.1	Triviality testing	32
5.2	Equivalence testing	35
5.3	Tracking homology classes	35
5.4	From testing homology class to estimating Betti numbers	36
5.5	Cycle detection	37
6	Cohomology and applications	38
6.1	An overview of cohomology	38
6.2	Cohomological frameworks for constructing r -cocycles	39
6.2.1	Constructing block encodings via projection onto $\ker(\delta^r)$	41
6.2.2	Manual construction via explicit representatives	43
6.3	Homology equivalence testing with cohomological frameworks	45
6.3.1	Constructing block encodings via projection onto $\ker(\delta^r)$	45
6.3.2	Manual construction via explicit representatives	45
7	Concluding remarks	46
A	Inverting ill-conditioned matrices	47
B	Stochastic rank estimation	48

1 Introduction

The field of topological data analysis (TDA) is a fast growing area that borrows tools from algebraic topology to analyze large scale data, such as graph networks. Typically, a collection of data points is given, where each data point can be a vector in a high dimensional space. Then, under appropriate conditions, e.g., imposing a metric that defines the distance between data points, certain pairwise connections between data points are formed. The objective is to analyze the potentially hidden structure of the resulting configuration. For example, one may ask how many loops (1-dimensional “holes”), voids (2-dimensional “holes”), holes (3-dimensional “holes”), etc., are present. Because standard graph theory only concerns low dimensional objects like vertices and edges, it is not sufficient to infer higher dimensional structure. On the other hand, homology theory, a major theory within algebraic topology, primarily concerns discrete objects such as 0-simplices (points or vertices), 1-simplices (edges), 2-simplices (triangles), and so on. Thus, it is intrinsically suitable for dealing with high dimensional objects and is capable of revealing the desired information.

At the same time, quantum computing is an emerging technology that leverages the core principles of quantum physics to store and process information. Major progress has been made since the first proposals for quantum computational frameworks [Man80, Ben80, Fey18]. Notable examples include Shor’s factorization algorithm [Sho99], Grover’s search algorithm [Gro96], and black-box property determination [Deu85, DJ92]. In addition, quantum algorithmic models have been shown to offer significant speedups over classical counterparts in solving linear equations [HHL09, CKS17] and simulating quantum systems [Llo96, BACS07, BC09, Ber14, BCK15, BCC⁺15, BCOW17, BSG⁺24]. Recently, the potential of quantum computing paradigms in machine learning and artificial intelligence has attracted significant attention [SP18, SBG⁺19, Sch19, SK19, SBSW20, SSM21, MNKF18, HCT⁺19, LMR13, LSI⁺20, BWP⁺17, RML14, RBWL18].

Altogether, the aforementioned works have demonstrated exciting progress in the field and have naturally motivated researchers to explore the potential of quantum computers for TDA. In fact, several significant results have been established. Lloyd, Garnerone, and Zanardi [LGZ16] introduced the first quantum algorithm—commonly referred to as the LGZ algorithm—for estimating Betti numbers, which are among the central quantities of interest in TDA. Their algorithm builds on several quantum primitives, such as quantum simulation techniques [BACS07], quantum phase estimation [Kit95], and the quantum search algorithm [Gro96]. Following this line of work, numerous subsequent studies have explored related directions [Hay22, MGB22, BSG⁺24, SUK24a, GSK⁺24, HCH24, SRZ⁺25, IGMD24, CK24, KK24, SUK24b, Ray24]. Some of these works aim to improve the LGZ algorithm in various aspects, while others seek to characterize the complexity classes of specific topological problems. Collectively, these developments lie at the intersection of topology, many-body physics, and quantum complexity theory. To some extent, these works have demonstrated the promise of quantum computers in tackling core challenges in TDA.

However, recent results present notable limitations for computing Betti numbers. Schmidhuber and Lloyd [SL23] showed that estimating Betti numbers for general graphs is NP-hard. Simultaneous and independent work by Crichigno and Kohler [CK24] significantly strengthened these hardness results for clique complexes: they proved that the counting version of this problem is #BQP-complete (which is polynomial-time equivalent to #P-complete), and that the decision variant with exponentially fine precision is QMA₁-hard. Combined with subsequent work by Rudolph [Rud24], this establishes that the problem is PSPACE-complete for clique complexes. Assuming widely believed complexity-theoretic conjectures, this implies that quantum computers are unlikely to efficiently solve the problem for generic inputs. As also suggested in [SL23], a quantum speed-up may still be achievable if the input representation of the graph or simplicial complex contains more information than mere pairwise connectivity between data points.

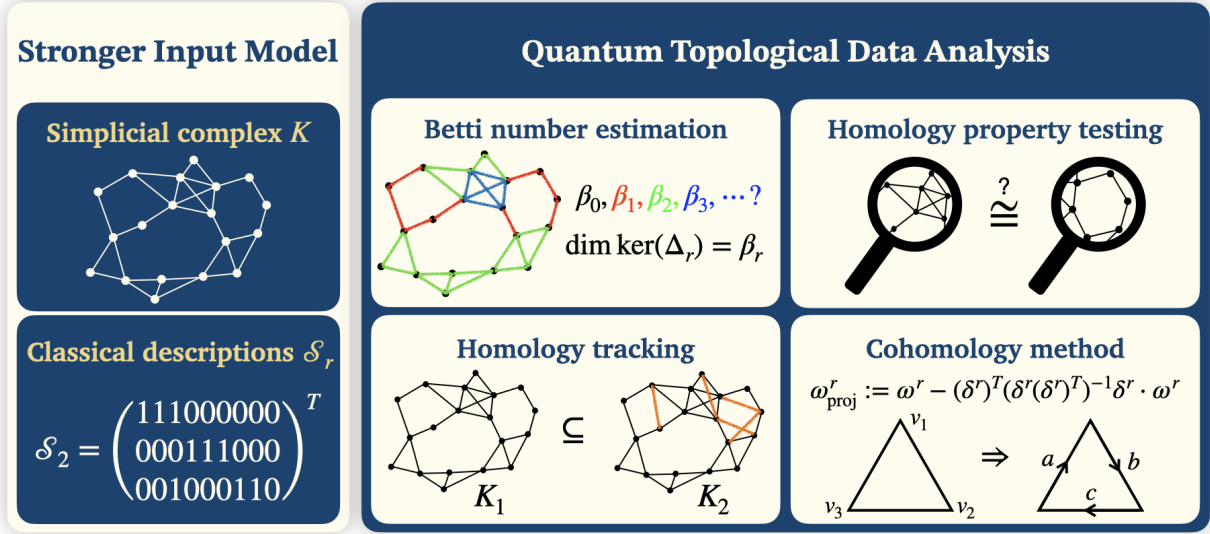


Figure 1: **Overview of our results.** We explore quantum algorithms for topological data analysis given explicit classical access to a simplicial complex K and its associated descriptions \mathcal{S}_r . Our results include algorithms for Betti number estimation β_r and persistent Betti number estimation, as well as homology property testing tasks such as triviality and equivalence testing. We further demonstrate applications to homology tracking and introduce a new cohomological approach based on differential operators.

Motivated by this result and the potential of quantum computers more broadly, we continue to explore quantum solutions to a variety of topology-related computational problems.

1.1 Organization of the paper

In [Section 2](#), we summarize our main results and present a high-level overview of the proposed quantum algorithms. [Section 3](#) introduces the necessary background on block encoding, algebraic topology, and prior work on quantum topological data analysis (TDA); readers familiar with these topics may skip this section.

Our quantum algorithms assume classical access to the combinatorial structure of a simplicial complex, namely, knowledge of which simplices are adjacent or serve as faces of higher-dimensional simplices (see [Section 4.1](#) for details). Based on this model, [Section 4](#) addresses the problem of estimating Betti numbers by constructing and analyzing the boundary operators associated with the complex. This framework is extended in [Section 4.3](#) to the estimation of persistent Betti numbers.

We then consider problems related to homology detection. (For reference, in our paper, the terms “homology detection” and “homology testing” may be used interchangeably, as they carry the same meaning.) [Section 5.1](#) presents a quantum algorithm to test whether a given cycle is homologous to zero, and [Section 5.2](#) generalizes this to decide whether two cycles are homologous. In [Section 6.2](#), we explore a cohomological approach to the same problem.

Next, we revisit Betti number estimation from a dynamic perspective in [Section 5.4](#), proposing an alternative quantum procedure. [Section 5.5](#) studies the problem of testing whether a given curve forms a valid cycle, and offers a quantum solution.

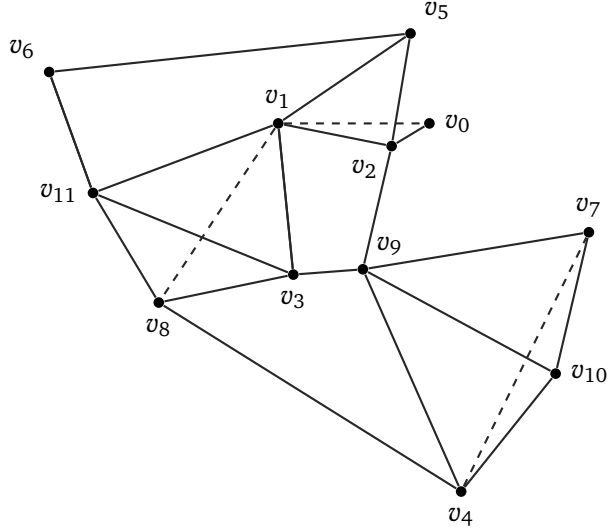


Figure 2: **A simplicial complex.** Combinatorial object built from simplices—vertices, edges, triangles, and higher-dimensional generalizations—that are glued together in a consistent way.

2 Overview and main results

In this section, we present an overview of our objectives, proposed methods, and main results. We also position our contributions within the broader context of quantum topological data analysis (TDA), highlighting their motivation and relevance to prior work. Each major computational task is formally introduced as a *Problem* statement, followed by a corresponding *Algorithm* illustrating the quantum algorithm designed to solve it. The algorithm’s performance is then formally captured in a *Theorem*. A rigorous development of the concepts, techniques, and proofs will be provided in the subsequent sections. We provide an overview of our results in Fig. 1.

2.1 Motivation and problem statement

In the context of TDA, one typically begins with a finite set of data points. By equipping the space with a suitable metric, pairwise distances between data points can be computed. Fixing a threshold (also referred to as a length scale) induces pairwise connectivity; for example, two points are declared connected if their distance lies below the threshold. This connectivity structure gives rise to a simplicial complex K (see Fig. 2 for an example). The central problem is the following:

What are the Betti numbers β_r of K ?

Several prior works [LGZ16, BSG⁺24, Hay22, MGB22], grounded in homology theory, have addressed this question under the assumption that access is provided via an oracle encoding pairwise connectivity among the data points. Although a rigorous treatment of the relevant algebraic topology will be provided in Section 3.2, we briefly review several essential concepts to facilitate the exposition of our main results.

- (i) An r -simplex is a fully connected subgraph on $(r+1)$ vertices (see Fig. 8 for an illustration). Thus, a 0-simplex is a vertex, a 1-simplex is an edge, and a 2-simplex is a triangle, and so on.
- (ii) A simplicial complex is a collection of simplices of various orders satisfying specific closure properties.

- (iii) A (formal) linear combination of r -simplices is referred to as an r -chain.
- (iv) The boundary operator ∂_r maps an r -simplex to a (formal) linear combination of $(r-1)$ -simplices.
- (v) An r -cycle is an r -chain c_r satisfying $\partial_r c_r = 0$.

Within homology theory, the set of r -simplices in K , denoted by $S_r^K = \{\sigma_{r_i}\}_{i=1}^{|S_r^K|}$, spans a vector space (alternatively, one may work with a finitely generated abelian group). An r -chain can then be represented as a vector in this space, and the boundary operator ∂_r acts as a linear map between the corresponding vector spaces. Given the family of boundary maps $\{\partial_r\}$, one can define the so-called r -th *combinatorial Laplacian* as

$$\Delta_r = \partial_{r+1} \partial_{r+1}^\dagger + \partial_r^\dagger \partial_r. \quad (2.1)$$

The r -th Betti number β_r is given by the dimension of the kernel of Δ_r , i.e., $\dim \ker(\Delta_r) = \beta_r$.

Given access to the aforementioned oracle, it is possible to construct Δ_r in a quantum manner and analyze its kernel, for instance, via the phase estimation algorithm, as demonstrated in [LGZ16]. A more detailed review of previous quantum algorithms [LGZ16, BSG⁺24, Hay22, MGB22] for estimating Betti numbers is provided in Fig. 9 and Section 3.3.

Despite these promising developments, a recent result by Schmidhuber and Lloyd [SL23] has established that computing Betti numbers is $\#P$ -hard, and even estimating them to within a given precision is NP-hard. This result effectively rules out the possibility of achieving an unconditional quantum advantage under such oracle-based input assumptions. As emphasized in [SL23], it is therefore crucial to explore alternative means of specifying simplicial complexes, beyond reliance solely on pairwise connectivity.

2.2 Input model setup

Motivated by this insight, we propose a modified input assumption. Let S_r^K denote the set of r -simplices in K , so that $K = \{S_r^K\}_{r=1}^n$, where n denotes the number of data points. We assume that a *classical description* of K is provided. By this, we mean that for each r , we are given classical access to a matrix \mathcal{S}_r of size $|S_{r-1}^K| \times |S_r^K|$. Each column i of \mathcal{S}_r , corresponding to an r -simplex σ_{r_i} , contains nonzero entries equal to 1, and the indices of these entries indicate the $(r-1)$ -simplices that are faces of σ_{r_i} . Equivalently, we may restate the problem as follows:

Problem 1 (Betti number estimation with classical description, see Section 4.2). *Given a simplicial complex K , specified via a classical description of its boundary matrices $\{\mathcal{S}_r\}$, estimate the Betti numbers $\{\beta_r\}$ of K . This formulation contrasts with prior oracle-based models; here, the simplicial complex is assumed to be explicitly given in classical form.*

2.3 Estimating Betti numbers

Given the matrices $\{\mathcal{S}_r\}$, one can efficiently recover the classical descriptions of the boundary maps $\{\partial_r\}$; see Section 3.2 for formal definitions. The overall procedure is summarized in Algorithm 1.

We define the quantity

$$\frac{\dim \ker(\Delta_r)}{|S_r^K|} = \frac{\beta_r}{|S_r^K|} \quad (2.2)$$

as the r -th *normalized Betti number*. The algorithm described above yields the following result:

Algorithm 1: Quantum algorithm for estimating normalized Betti numbers

- 1 **Input:** Classical description of a simplicial complex $K = \{S_r^K\}_{r=1}^n$
 - 2 Construct boundary maps ∂_r from K
 - 3 Compute a block-encoding of $\partial_r^\dagger \partial_r / ((r+1)|S_r^K|)$
 - 4 Construct a block-encoding of the combinatorial Laplacian $\Delta_r / (2(r+1)(r+2)|S_r^K||S_{r+1}^K|)$
 - 5 Estimate $\text{rank}(\Delta_r) / |S_r^K|$ using stochastic rank estimation
 - 6 Compute $\beta_r / |S_r^K| = 1 - \text{rank}(\Delta_r) / |S_r^K|$
 - 7 **Output:** Normalized Betti number $\beta_r / |S_r^K|$
-

Theorem 2.1 (Time complexity of estimating (normalized) Betti numbers, see [Section 4.2](#)). *Let $\{S_r\}$ be the classical specification of a simplicial complex K . Then, the r -th normalized Betti number $\beta_r / |S_r^K|$ can be estimated to additive precision ϵ with time complexity*

$$\mathcal{O}\left(\frac{\log(r|S_r^K|) \log(r^2|S_r^K||S_{r+1}^K|)}{\epsilon^2}\right). \quad (2.3)$$

Moreover, the r -th Betti number β_r can be estimated to multiplicative precision δ with time complexity

$$\mathcal{O}\left(\frac{\log(r|S_r^K|) \log(r^2|S_r^K||S_{r+1}^K|)|S_r^K|^2}{\delta^2 \beta_r^2}\right). \quad (2.4)$$

As we summarize in [Section 3.3](#), to the best of our knowledge, the state-of-the-art quantum algorithm (referred to as the LGZ algorithm) achieves the following time complexities for estimating normalized Betti numbers (to additive precision ϵ) and unnormalized Betti numbers (to multiplicative precision δ), respectively:

$$\mathcal{O}\left(\frac{1}{\epsilon} \cdot \left(n^2 \sqrt{\frac{\binom{n}{r+1}}{|S_r^K|}} + n\kappa\right)\right), \quad \mathcal{O}\left(\frac{1}{\delta} \cdot \left(n^2 \sqrt{\frac{\binom{n}{r+1}}{\beta_r}} + n\kappa \sqrt{\frac{|S_r^K|}{\beta_r}}\right)\right), \quad (2.5)$$

where κ denotes the condition number of the combinatorial Laplacian Δ_r .

As can be seen, with respect to the normalized Betti numbers $\beta_r / |S_r^K|$, the LGZ algorithm is efficient only when $|S_r^K|$ is sufficiently large; that is, when the simplicial complex is dense. In the best-case scenario where the ratio $\binom{n}{r+1} / |S_r^K|$ is $\mathcal{O}(1)$, the LGZ algorithm achieves time complexity $\mathcal{O}(n^2 + n\kappa)$.

In contrast, as long as $|S_r^K| \in \mathcal{O}(\text{poly}(n))$, our algorithm achieves time complexity $\mathcal{O}(\text{poly}(\log(n)))$, thus exhibiting a *superpolynomial* speed-up over the LGZ algorithm. The advantage becomes even more pronounced when the ratio $\binom{n}{r+1} / |S_r^K|$ is itself in $\mathcal{O}(\text{poly}(n))$.

In the *sparse regime*, where $|S_r^K| \ll \binom{n}{r+1}$, the ratio

$$\frac{\binom{n}{r+1}}{|S_r^K|} \approx \binom{n}{r+1}, \quad (2.6)$$

and the LGZ algorithm suffers from large overhead. Meanwhile, the classical specification cost in our approach remains $\mathcal{O}(\log(r|S_r^K|) \cdot \log(r^2|S_r^K||S_{r+1}^K|))$, which is significantly smaller than

$$\mathcal{O}\left(\log\left(r \binom{n}{r+1}\right) \cdot \log\left(r^2 \binom{n}{r+1} \binom{n}{r+2}\right)\right). \quad (2.7)$$

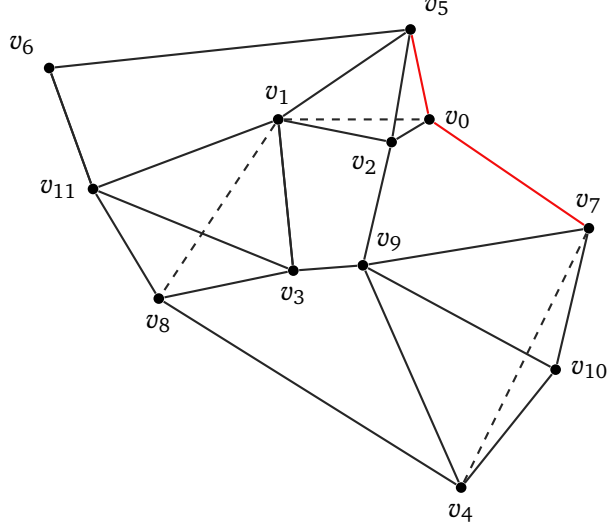


Figure 3: **Illustration of persistent Betti numbers.** In this figure, $[v_1, v_2, v_9, v_3]$ forms a 1-dimensional hole (loop) in the initial complex, while $[v_0, v_2, v_9, v_7]$ does not form a loop at the current threshold. As the threshold increases, two new edges, $[v_0, v_5]$ and $[v_0, v_7]$ (red), are added. These additions complete a new loop involving $[v_0, v_2, v_9, v_7]$, which was not present before. Persistent Betti numbers capture such topological features (holes) that emerge and persist across multiple scales.

Algorithm 2: Quantum algorithm for estimating normalized persistent Betti numbers

- 1 **Input:** Classical descriptions of two simplicial complexes $K_1 \subseteq K_2$
 - 2 Construct boundary maps $\partial_r^{K_1}$ and $\partial_r^{K_2}$
 - 3 Construct block-encodings of $\partial_r^\dagger \partial_r$ for both complexes
 - 4 Build block-encoding of r -th persistent combinatorial Laplacian

$$\Delta_r^{K_1, K_2} = \partial_{r+1}^{K_1, K_2} (\partial_{r+1}^{K_1, K_2})^\dagger + (\partial_r^{K_1})^\dagger \partial_r^{K_1}$$
 - 5 Estimate $\text{rank}(\Delta_r^{K_1, K_2}) / |S_r^K|$ using stochastic rank estimation
 - 6 Compute $\beta_r^{\text{persistent}} / |S_r^K| = 1 - \text{rank}(\Delta_r^{K_1, K_2}) / |S_r^K|$
 - 7 **Output:** Normalized persistent Betti number $\beta_r^{\text{persistent}} / |S_r^K|$
-

Therefore, if $\binom{n}{r+1} \in \mathcal{O}(\text{poly}(n))$, our algorithm achieves a superpolynomial speed-up. If $\binom{n}{r+1} \in \exp(n)$, the resulting speed-up becomes *nearly exponential*.

In terms of estimating the (unnormalized) Betti numbers β_r , both algorithms achieve their best performance when $\beta_r \approx |S_r^K|$, i.e., when the normalized Betti number is constant. In this regime, our algorithm exhibits time complexity $\mathcal{O}(\log(r|S_r^K|) \cdot \log(r^2|S_r^K||S_{r+1}^K|))$, while the LGZ algorithm yields

$$\mathcal{O}\left(n^2 \sqrt{\frac{\binom{n}{r+1}}{\beta_r}}\right) \approx \mathcal{O}\left(n^2 \sqrt{\frac{\binom{n}{r+1}}{|S_r^K|}}\right). \quad (2.8)$$

Thus, the comparison remains similar: our algorithm achieves a superpolynomial speed-up in the dense regime and a near-exponential speed-up in the sparse regime.

2.4 Estimating persistent Betti numbers

We remark that the above result assumes a fixed simplicial complex K , denoted hereafter by K_1 , constructed from pairwise connectivity under a given threshold (or length scale). As the threshold increases, additional connections are formed among the data points, yielding a denser simplicial complex K_2 .

It is straightforward to verify that $K_1 \subseteq K_2$, since all connections present in K_1 are preserved in K_2 , while K_2 may contain additional pairwise connections. While Betti numbers quantify the “holes” within a given complex (e.g., K_1), the *persistent Betti numbers* capture the topological features that persist from the earlier complex (corresponding to a smaller threshold) to the later one (with a larger threshold). Our objective is thus to compute the persistent Betti numbers associated with the inclusion $K_1 \subseteq K_2$.

This problem was previously considered in [Hay22], where the input model assumes oracle access encoding pairwise connectivity of the underlying data points at two distinct thresholds—essentially requiring two separate oracles for K_1 and K_2 . As before, we depart from the oracle-based model and instead assume that classical descriptions of K_1 and K_2 are available. This leads us to the following reformulation of the computational task:

Problem 2 (Persistent Betti number estimation with classical description, see Section 4.3). *Given two simplicial complexes $K_1 \subseteq K_2$, specified via classical boundary matrix descriptions $\{\mathcal{S}_r^{K_1}\}$ and $\{\mathcal{S}_r^{K_2}\}$, estimate the persistent Betti numbers associated with the inclusion $K_1 \subseteq K_2$.*

Our algorithm builds on the method proposed in [Hay22]. To estimate persistent Betti numbers, one must consider the *persistent combinatorial Laplacian*. Recall that the standard r -th combinatorial Laplacian is defined by Eq. (2.1). The r -th persistent combinatorial Laplacian is given by

$$\Delta_r^{K_1, K_2} = \partial_{r+1}^{K_1, K_2} (\partial_{r+1}^{K_1, K_2})^\dagger + (\partial_r^{K_1})^\dagger \partial_r^{K_1} \quad (2.9)$$

where $\partial_{r+1}^{K_1, K_2}$ denotes the restriction of $\partial_{r+1}^{K_2}$ to an appropriate subspace. A more detailed discussion of this operator, including the construction of the first term, appears in Section 4.3. We emphasize here that the spectrum of $\Delta_r^{K_1, K_2}$ encodes the persistent Betti numbers; specifically, $\beta_r^{\text{persistent}} = \dim \ker(\Delta_r^{K_1, K_2})$. While the full algorithmic procedure is deferred to Section 4.3, we summarize the essential steps in Algorithm 2 and yields the following complexity result:

Theorem 2.2 (Time complexity of estimating (normalized) persistent Betti numbers, see Section 4.3). *Let $K_1 \subseteq K_2$ be simplicial complexes with classical specifications given by $\{\mathcal{S}_r^{K_1}\}, \{\mathcal{S}_r^{K_2}\}$. Then, the r -th normalized persistent Betti number $\beta_r^{\text{persistent}} / |\mathcal{S}_r^{K_1}|$ can be estimated to additive precision ϵ , with time complexity*

$$\mathcal{O}\left(\frac{\log\left(r^2 |\mathcal{S}_r^{K_1}| (|\mathcal{S}_{r+1}^{K_2}| - |\mathcal{S}_{r+1}^{K_1}|)\right) \left(\log^2(1/\epsilon) \log\left(r (|\mathcal{S}_{r+1}^{K_2}| - |\mathcal{S}_{r+1}^{K_1}|)\right) + \log\left(r |\mathcal{S}_r^{K_1}|\right)\right)}{\epsilon^2}\right). \quad (2.10)$$

Furthermore, the r -th persistent Betti number $\beta_r^{\text{persistent}}$ can be estimated to multiplicative accuracy δ , with time complexity

$$\mathcal{O}\left(\frac{|\mathcal{S}_r^{K_1}|^2 \log\left(r^2 |\mathcal{S}_r^{K_1}| (|\mathcal{S}_{r+1}^{K_2}| - |\mathcal{S}_{r+1}^{K_1}|)\right) \left(\log^2(1/\epsilon) \log\left(r (|\mathcal{S}_{r+1}^{K_2}| - |\mathcal{S}_{r+1}^{K_1}|)\right) + \log\left(r |\mathcal{S}_r^{K_1}|\right)\right)}{\delta^2 (\beta_r^{\text{persistent}})^2}\right). \quad (2.11)$$

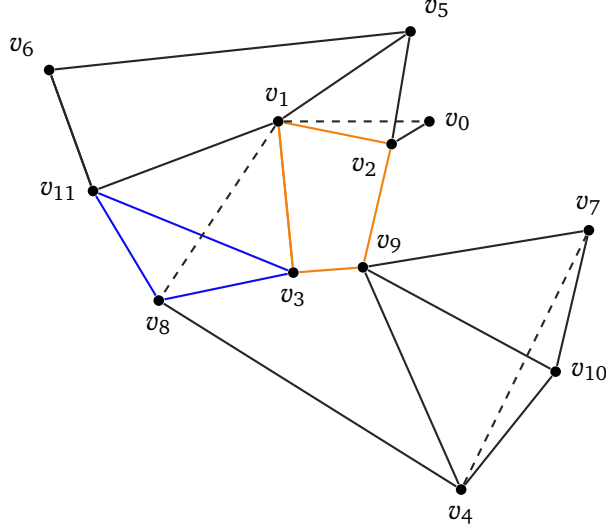


Figure 4: **Non-trivial vs. Trivial loops/cycles.** A simplicial complex is given. Both $[v_1, v_2, v_3, v_9]$ (orange) and $[v_3, v_8, v_{11}]$ (blue) form loops. However, the blue loop bounds a filled-in triangle and is therefore homologous to zero—it is trivial in homology. In contrast, the orange loop does not bound any region and thus represents a non-trivial homology class. The first Betti number counts such distinct, linearly independent non-trivial classes.

To compare, we quote the following complexity bounds from [Hay22] for estimating the r -th normalized persistent Betti number to additive accuracy ϵ , and the persistent Betti number to multiplicative accuracy δ , respectively:

$$\mathcal{O}\left(\frac{\log(1/\epsilon)}{\epsilon^2} \cdot \left(rn^2 \sqrt{\frac{\binom{n}{r+1}}{|S_r^{K_1}|}} + r^4 n^8 \log(1/\epsilon)\right)\right), \quad (2.12)$$

$$\mathcal{O}\left(\frac{|S_r^{K_1}|^{3/2}}{\delta^2 (\beta_r^{\text{persistent}})^2} \cdot \left(rn^2 \sqrt{\binom{n}{r+1}} + r^4 n^8 |S_r^{K_1}|^{1/2} \log\left(\frac{|S_r^{K_1}|}{\delta \beta_r^{\text{persistent}}}\right)\right) \log\left(\frac{|S_r^{K_1}|}{\delta \beta_r^{\text{persistent}}}\right)\right). \quad (2.13)$$

If the difference $|S_{r+1}^{K_2}| - |S_{r+1}^{K_1}|$ is small—e.g., of order $\mathcal{O}(1)$ —then the complexity comparison becomes essentially the same as that discussed previously between our algorithm and the LGZ algorithm for estimating Betti numbers. In this setting, the same conclusion applies: our method achieves a *superpolynomial* speed-up in the sparse regime and a *near-exponential* speed-up in the dense regime.

2.5 Testing for trivial homology classes

Thus far, we have considered the estimation of (normalized) Betti numbers and persistent Betti numbers, quantities that encapsulate topological invariants of the underlying simplicial complex. Motivated by this, we now turn to a related foundational task in algebraic topology that extends beyond the computation of Betti numbers. Subsequently, we also discuss how it can be applied to TDA. Specifically, we consider the following:

Problem 3 (Homology triviality testing with classical description, see Section 5.1). *Given the classical description $\{S_r\}$ of a simplicial complex K , and an r -cycle c_r , determine whether c_r is homologous to zero.*

Algorithm 3: Quantum algorithm for homology triviality testing

- 1 **Input:** Simplicial complex $K = \{S_r^K\}_{r=1}^n$, input r -cycle c_r
 - 2 Construct boundary map ∂_{r+1}
 - 3 Block-encode operator $\partial_{r+1}^\dagger \partial_{r+1} / ((r+2)|S_{r+1}^K|)$
 - 4 Estimate $\text{rank}(\partial_{r+1})/|S_{r+1}^K|$ and $\text{rank}([\partial_{r+1}|c_r])/(|S_{r+1}^K| + 1)$ using stochastic rank estimation
 - 5 **if** $\text{rank}(\partial_r) = \text{rank}([\partial_r|c_r])$ **then**
 - 6 | **return** “ c_r is homologous to zero”
 - 7 **else**
 - 8 | **return** “ c_r is not homologous to zero”
 - 9 **Output:** Decision whether c_r is homologous to zero
-

We refer to Fig. 4 for an illustration of our objective. Our solution to Problem 3 relies on the algebraic structure of chain complexes: r -simplices serve as a basis for a vector space, and an r -cycle c_r is a (formal) linear combination of r -simplices, which can be represented as a vector in this space.

A necessary and sufficient condition for c_r to be homologous to zero is that the following linear equation admits a solution:

$$\partial_{r+1}c_{r+1} = c_r, \quad (2.14)$$

which directly follows from the definition: an r -cycle is homologous to zero if it is the boundary of some $(r+1)$ -chain (see Section 3.2 for further details).

To determine whether a solution exists, it suffices to check whether the matrices ∂_{r+1} and $[\partial_{r+1}|c_r]$ have the same rank. A more detailed discussion is provided in Section 5.1, and we summarize our algorithmic approach in Algorithm 3.

Theorem 2.3 (Time complexity of testing homology triviality, see Section 5.1). *Let K be a simplicial complex with classical description $\{S_r\}$. Given an r -cycle c_r , whether it is homologous to zero can be determined with high probability in time complexity*

$$\mathcal{O}\left(\frac{\log(r|S_{r+1}^K|) \log((r+2)|S_{r+1}^K| + L)|S_{r+1}^K|^2}{(\text{rank}(\partial_{r+1}))^2}\right), \quad (2.15)$$

where L is the bit-length required to describe the cycle c_r . This bound assumes that both $\text{rank}(\partial_{r+1})$ and $\text{rank}([\partial_{r+1}|c_r])$ can be estimated to constant multiplicative accuracy.

A naive classical approach to solve the same problem is to compute the ranks of ∂_{r+1} and $[\partial_{r+1}|c_r]$ via Gaussian elimination, which incurs a time complexity of $\mathcal{O}(|S_{r+1}^K|^3)$. Therefore, in order for our quantum algorithm to exhibit an potential exponential speed-up over the classical method, it is necessary for the rank of ∂_{r+1} to be large—ideally, of the same order as $|S_{r+1}^K|$. This condition is met when the Betti number β_{r+1} is much smaller than $|S_{r+1}^K|$, i.e., $\beta_{r+1} \ll |S_{r+1}^K|$.

In this regime, our algorithm achieves its best performance. Notably, this regime is the opposite of that of previous quantum algorithms for estimating Betti numbers (see Theorem 2.1 and Theorem 2.2), which perform better when Betti numbers are large.

2.6 Testing homology equivalence

Beyond checking whether a single cycle is homologous to zero, the above algorithm can be naturally extended to test whether two given r -cycles are homologous to each other.

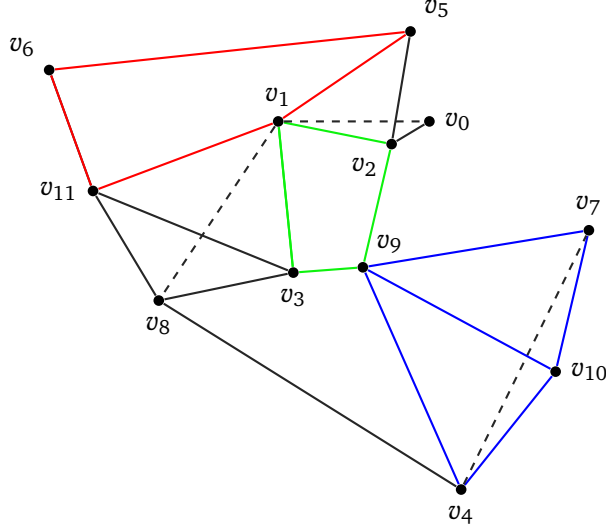


Figure 5: **Different homology classes.** A simplicial complex is given. Both $[v_1, v_2, v_9, v_3]$ (green) and $[v_1, v_5, v_6, v_{11}]$ (red) are non-trivial loops, but they are not homologous to each other. In the language of homology theory (see Section 3.2), their (formal) sum does not form the boundary of any (formal) sum of triangles. On the other hand, $[v_7, v_9, v_{10}]$ and $[v_4, v_9, v_{10}]$ (blue) are homologous (in fact, both are homologous to zero), since their (formal) sum forms the boundary of $[v_4, v_9, v_{10}] + [v_7, v_9, v_{10}]$. More generally, our goal is to test whether two given r -cycles belong to the same homology class.

Algorithm 4: Quantum algorithm for homology equivalence testing

- 1 **Input:** Simplicial complex $K = \{S_r^K\}_{r=1}^n$, two r -cycles c_{r_1}, c_{r_2}
 - 2 Construct boundary map ∂_{r+1}
 - 3 Block-encode operator $\partial_{r+1}^\dagger \partial_{r+1} / ((r+2)|S_{r+1}^K|)$
 - 4 Estimate $\text{rank}(\partial_{r+1})/|S_{r+1}^K|$ and $\text{rank}([\partial_{r+1}(c_{r_1} - c_{r_2})])/(|S_{r+1}^K| + 1)$ using stochastic rank estimation
 - 5 Estimate $\text{rank}(\partial_r)$ and $\text{rank}([\partial_r(c_{r_1} - c_{r_2})])$
 - 6 **if** $\text{rank}(\partial_r) = \text{rank}([\partial_r(c_{r_1} - c_{r_2})])$ **then**
 - 7 | **return** “ $c_{r_1} \sim c_{r_2}$ (homology equivalent)”
 - 8 **else**
 - 9 | **return** “ $c_{r_1} \not\sim c_{r_2}$ (not equivalent)”
 - 10 **Output:** Decide if $c_{r_1} \sim c_{r_2}$
-

Problem 4 (Homology equivalence testing with classical description, see Section 5.2). *Given a simplicial complex K , specified via a classical description of its boundary matrices $\{S_r\}$, and two r -cycles c_1 and c_2 represented as explicit vectors in the r -chain space, determine whether c_1 and c_2 are homologous.*

See Fig. 5 for an illustration of distinct homology classes and the goal of this task. We first recall the basic translative property of homology: if $c_{r_1} \sim c_{r_2}$ and $c_{r_2} \sim c_{r_3}$, then $c_{r_1} \sim c_{r_3}$. To test the relation $c_{r_1} \sim c_{r_2}$, our algorithm again relies on two key facts: (i) c_{r_1} and c_{r_2} are known vectors, and (ii) a sufficient condition for their homology is that the linear system

$$\partial_{r+1} c_{r+1} = c_{r_1} - c_{r_2} \tag{2.16}$$

has a solution. This follows directly from the definition that two r -cycles are homologous if their difference is the boundary of an $(r+1)$ -chain.

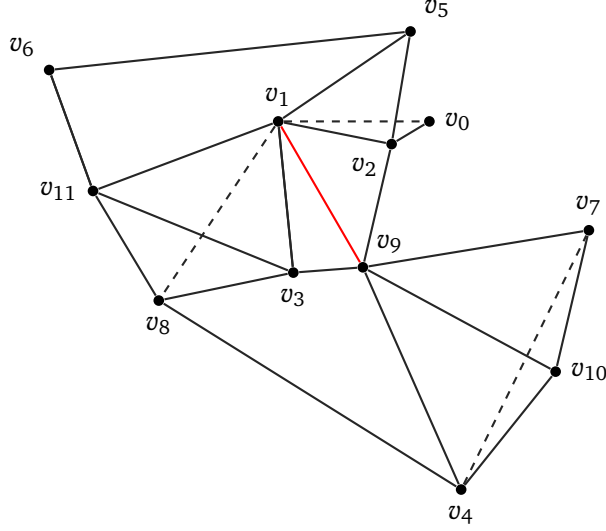


Figure 6: **Illustration of a potential application of homology class detection.** In the complex K_1 (excluding the red edge $[v_1, v_9]$), the cycle $[v_1, v_2, v_9, v_3]$ forms a nontrivial loop (as can be determined using [Theorem 2.3](#)). However, once the edge $[v_1, v_9]$ (red) is added to the complex, the cycle $[v_1, v_2, v_9, v_3]$ becomes trivial, i.e., homologous to zero. The central idea of our proposal for homology tracking is to examine the behavior of a particular cycle across different stages of the filtration, which may reveal additional topological information about the underlying data set.

Since the classical descriptions of c_{r_1} and c_{r_2} are given, we can construct the difference vector $c_{r_1} - c_{r_2}$ efficiently. Then, testing whether the system admits a solution reduces to checking whether

$$\text{rank}(\partial_{r+1}) = \text{rank}([\partial_{r+1}|(c_{r_1} - c_{r_2})]). \quad (2.17)$$

This allows us to reuse the same quantum procedure outlined in [Algorithm 3](#), with essentially the same time complexity:

Theorem 2.4 (Time complexity of testing homology equivalence, see [Section 5.2](#)). *Given a simplicial complex K with classical description $\{S_r\}$, whether two r -cycles c_{r_1} and c_{r_2} are homologous to each other can be determined with high probability in time complexity*

$$\mathcal{O}\left(\frac{\log(r|S_{r+1}^K|) \cdot \log((r+2)|S_{r+1}^K| + L)|S_{r+1}^K|^2}{(\text{rank}(\partial_{r+1}))^2}\right), \quad (2.18)$$

where L denotes the larger bit-length of c_{r_1} and c_{r_2} . This bound assumes that both $\text{rank}([\partial_{r+1}|(c_{r_1} - c_{r_2})])$ and $\text{rank}(\partial_{r+1})$ can be estimated to constant multiplicative accuracy.

As with the zero-homology case, if the rank of ∂_{r+1} is large (e.g., $\approx |S_{r+1}^K|$), our quantum algorithm achieves an exponential speed-up over the classical method, which again requires Gaussian elimination to compute the ranks of ∂_{r+1} and $[\partial_{r+1}|(c_{r_1} - c_{r_2})]$.

2.7 Applications to topological data analysis

2.7.1 Tracking homology classes

As discussed above, estimating Betti numbers is a central task in topological data analysis (TDA), as they encode intrinsic topological features of the underlying data set. However, it has been shown in [\[SL23\]](#) that

Algorithm 5: Quantum algorithm for Betti number estimation via homology property testing

```
1 Input: Simplicial complex  $K$ , candidate  $r$ -cycles  $c_{r_1}, \dots, c_{r_s}$ 
2 Initialize representative set  $\mathcal{H} = \{c_{r_1}\}$ 
3 for  $i = 2$  to  $s$  do
4   foreach  $c_{r_j}^h \in \mathcal{H}$  do
5     Test homology equivalence between  $c_{r_j}^h$  and  $c_{r_i}$  using Algorithm 4 if equivalent then
6     | break inner loop (already represented)
7   if no equivalent representative found then
8   | Add  $c_{r_i}$  to  $\mathcal{H}$ 
9 Form matrix  $M = [c_{r_1}^h, c_{r_2}^h, \dots, c_{r_p}^h]$  from representatives in  $\mathcal{H}$ 
10 Estimate  $\text{rank}(M)$  via stochastic rank estimation
11 Compute  $\beta_r = \text{rank}(M)$ 
12 Output: Betti number estimate  $\beta_r$ 
```

this problem is NP-hard, and therefore admits no efficient algorithm under widely believed complexity-theoretic assumptions. In addition to motivating our earlier attempt to consider alternative input models for Betti number estimation, this result also inspires us to explore a different direction in which quantum computation may prove useful for TDA.

In the context of persistent Betti numbers, one typically considers a simplicial complex K_1 constructed at a given threshold (or length scale), and another complex K_2 obtained at a higher threshold. Rather than analyzing the persistent Betti numbers directly, we propose to track the evolution of a specific homology class and examine its behavior across the filtration, leveraging our algorithms for homology class detection described above. An illustration of this proposal is provided in [Fig. 6](#).

Generally, for an r -cycle c_r , if it is not homologous to zero in K_1 (i.e., it represents a nontrivial homology class), but becomes homologous to zero in K_2 , this may indicate that the cycle—or the entire class it represents—is topological noise. Subsequently, one may continue to track the behavior of c_r in a further complex K_3 , constructed at a higher threshold or length scale.

More generally, given two cycles c_{r_1} and c_{r_2} , one can track their homology relation across the filtration. If they are homologous in K_1 but no longer homologous in K_2 or K_3 , this may signal a change in the topological structure of the data. Therefore, this approach of tracking homology classes across varying thresholds or length scales provides an alternative perspective for extracting topological insights from the underlying data set.

2.7.2 An alternative approach to Betti number estimation

In our earlier discussion, as well as in several related works [[SL23](#), [LGZ16](#), [Hay22](#), [BSG⁺24](#), [MGB22](#)], the quantum algorithm for estimating (normalized) Betti numbers relies on the basic identity $\beta_r = \dim \ker(\Delta_r)$. Accordingly, the goal of these approaches (see, e.g., [Algorithm 1](#)) is to construct the combinatorial Laplacian Δ_r and then estimate the dimension of its kernel. This remains one of the most standard methods for computing Betti numbers of a given complex.

As stated in [Theorem 2.1](#), the complexity of estimating the r -th Betti number of a complex K scales as approximately $\sim |S_r^K|/\beta_r$. Thus, for the algorithm to be efficient, it is necessary that β_r is comparable to $|S_r^K|$ —that is, the complex must exhibit *large* Betti numbers. At first glance, this might seem counterintuitive: higher Betti numbers correspond to a more intricate topological structure, characterized by a larger number of “holes”. Motivated by this observation, we investigate the opposite

regime—when β_r is small—and explore whether an efficient algorithm can still be devised. Interestingly, such an algorithm does exist, and it naturally emerges from our earlier procedure for testing whether two given cycles are homologous.

To describe the method, we recall a foundational definition: the r -th homology group of a simplicial complex is given by

$$H_r = \frac{\ker \partial_r}{\text{im } \partial_{r+1}}, \quad (2.19)$$

and the r -th Betti number is defined as the dimension of this quotient space. A more formal treatment is provided in [Section 3.2](#) and [Section 3.3](#). By definition, the dimension of a vector space is equal to the maximal number of linearly independent vectors contained in it. This observation leads to a natural strategy: we attempt to identify elements of H_r and count how many are linearly independent, from which β_r can be inferred.

To obtain elements of H_r , we begin by noting that the quotient space $\ker \partial_r / \text{im } \partial_{r+1}$ defines an equivalence relation on $\ker \partial_r$ —the space of r -cycles. Two r -cycles are considered equivalent (i.e., homologous) if their difference lies in $\text{im } \partial_{r+1}$. This homology relation was previously used and formalized in our algorithm for testing equivalence of cycles (see, e.g., [Eq. \(2.16\)](#)).

Based on this, we proceed as follows: we randomly sample a collection of r -cycles, and then employ the algorithm outlined in [Algorithm 4](#) to determine their pairwise homology relations. Homologous cycles are grouped together, and one representative from each class is retained. The final step is to estimate the number of linearly independent representatives among these, which corresponds to the number of independent homology classes, i.e., the Betti number. A schematic summary of this approach is provided in [Algorithm 5](#).

A detailed analysis of the above algorithm is provided in [Section 5.4](#). The complexity of estimating the normalized rank

$$\frac{1}{p} \text{rank}[c_{r_1}^h, c_{r_2}^h, \dots, c_{r_p}^h] \quad (2.20)$$

to additive accuracy ϵ is given by

$$\mathcal{O}\left(s \cdot \frac{\log(r|S_{r+1}^K|) \log((r+2)|S_{r+1}^K| + L)|S_{r+1}^K|^2}{(\text{rank}(\partial_{r+1}))^2}\right) + \mathcal{O}\left(\frac{\log(p|S_r^K|)}{\epsilon^2}\right). \quad (2.21)$$

To obtain a multiplicative error δ in estimating

$$\text{rank}[c_{r_1}^h, \dots, c_{r_p}^h], \quad (2.22)$$

yielding the following complexity:

$$\mathcal{O}\left(s \cdot \frac{\log(r|S_{r+1}^K|) \log((r+2)|S_{r+1}^K| + L)|S_{r+1}^K|^2}{(\text{rank}(\partial_{r+1}))^2}\right) + \mathcal{O}\left(\frac{p^2 \log(p|S_r^K|)}{\delta^2 \beta_r^2}\right). \quad (2.23)$$

Here, the factor s in the first term arises from Step 2 of [Algorithm 5](#).

We now discuss the complexity in comparison to the classical method. As mentioned earlier, homology equivalence testing can be performed classically using Gaussian elimination. Similarly, the final step of computing [Eq. \(2.22\)](#) can also be done classically by Gaussian elimination. The total classical complexity is thus $\mathcal{O}(|S_{r+1}^K|^3 + p^3)$.

In order to achieve exponential quantum speed-up with respect to both $|S_{r+1}^K|$ and p , it is sufficient that $\text{rank}(\partial_{r+1}) \approx |S_{r+1}^K|$, and $\beta_r \approx p$. As previously discussed and further elaborated in [Section 5.1](#)

Algorithm 6: Quantum algorithm for nontrivial cycle detection

- 1 **Input:** Simplicial complex $K = \{S_r^K\}_{r=1}^n$, r -chain c_r
 - 2 Construct boundary map ∂_{r+1} from K
 - 3 Block-encode operator $\partial_{r+1}^\dagger \partial_{r+1} / ((r+2)|S_{r+1}^K|)$
 - 4 Apply block encoding to state $|0\rangle |c_r\rangle$
 - 5 Measure ancilla qubit
 - 6 **if** measurement outcome is $|0\rangle$ *with high probability* **then**
 - 7 | Output: c_r is likely **not** a cycle
 - 8 **else**
 - 9 | Output: c_r is likely a cycle
 - 10 **Output:** Whether c_r is likely a cycle
-

and Section 5.2, the first condition is satisfied when $\beta_{r+1} \ll |S_{r+1}^K|$, i.e., the complex K has low $(r+1)$ -st Betti number. If β_r is also small, then in principle only a small number of representative cycles from H_r are required, which implies that both s and p can remain small. Consequently, the second condition is satisfied, and the quantum algorithm achieves optimal efficiency in this regime.

2.8 Detecting nontrivial cycles

As discussed above, the core notion in homology theory is that of a *cycle*. In low dimensions, such as in the case of one-dimensional loops, it is straightforward to visualize cycles—for example, those highlighted in Fig. 2, Fig. 3, and Fig. 4. In these cases, determining whether a given curve is a cycle amounts to checking whether it is closed. However, in higher dimensions, such intuition does not hold, and it becomes nontrivial to decide whether a given object constitutes a cycle.

The question of interest is therefore the following: given an r -dimensional curve—more formally, an r -chain c_r (see Section 3.2 for the formal definition)—how can one determine whether it is a cycle?

Problem 5 (Cycle detection with classical description, see Section 5.5). *Given a simplicial complex K , specified via a classical description of its boundary matrices $\{S_r\}$, and an r -chain c_r explicitly described as a vector, determine whether c_r is an r -cycle.*

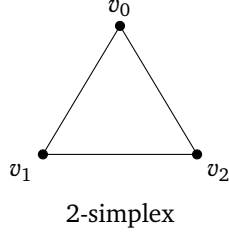
By definition, an r -cycle is an r -chain that lies in the kernel of the boundary map, i.e., it satisfies $\partial_r c_r = 0$. Thus, the problem reduces to verifying whether $c_r \in \ker(\partial_r)$. Recalling the algorithms in Algorithm 1 and Algorithm 2, and in particular Lemma 4.1, we have access to a block encoding of the Hermitian operator

$$\frac{\partial_{r+1}^\dagger \partial_{r+1}}{(r+2)|S_{r+1}^K|}. \quad (2.24)$$

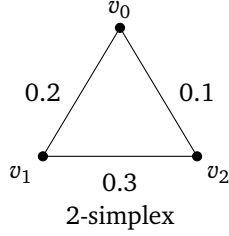
Our proposal is to use this block encoding and apply the resulting unitary to the normalized input state $|c_r\rangle := c_r / \|c_r\|$ (with appropriate ancilla). Measuring the ancillary qubits yields information about whether c_r lies in the kernel of ∂_r , i.e., whether it is a cycle, with some success probability. The detailed procedure is illustrated in Algorithm 6.

Theorem 2.5 (Time complexity of detecting cycles, see Section 5.5). *Let K be a simplicial complex specified by the classical description $\{S_r\}$. Then, given an r -chain c_r , there exists a quantum algorithm that determines whether c_r is a cycle with success probability $1 - \eta$, in time complexity*

$$\mathcal{O}\left(\frac{\log(r|S_r^K|)}{\eta}\right). \quad (2.25)$$



a – Homology detects the presence of 1-simplices (edges) enclosing a 2-simplex.



b – Cohomology assigns scalar values to the 1-simplices.

Figure 7: **Illustration of the conceptual distinction between homology and cohomology.** While homology captures the presence of cycles (e.g., bounding a 2-simplex), cohomology assigns values to simplices, allowing for more refined algebraic structure.

Algorithm 7: Cohomological quantum algorithm for homology equivalence testing

- 1 **Input:** Simplicial complex $K = \{S_r^K\}_{r=1}^n$, two r -cycles c_{r_1}, c_{r_2}
- 2 Construct coboundary map δ^r from K
- 3 Choose a random r -cochain ω^r
- 4 Project ω^r onto cocycle space:

$$\omega_{\text{proj}}^r = \omega^r - (\delta^r)^T (\delta^r (\delta^r)^T)^{-1} \delta^r \omega^r$$

- 5 Evaluate ω_{proj}^r on cycles c_{r_1} and c_{r_2}
 - 6 **if** $\omega_{\text{proj}}^r(c_{r_1}) = \omega_{\text{proj}}^r(c_{r_2})$ **then**
 - 7 Output: $c_{r_1} \sim c_{r_2}$ (homologous)
 - 8 **else**
 - 9 Output: $c_{r_1} \not\sim c_{r_2}$ (not homologous)
 - 10 **Output:** Decide if $c_{r_1} \sim c_{r_2}$ (homology equivalent)
-

A classical solution to the cycle detection problem is to compute the product $\partial_r c_r$ and examine each entry to determine whether it is zero. This leads to classical complexity $\mathcal{O}(|S_r^K|)$. Hence, our quantum algorithm achieves exponential speed-up in terms of query complexity, at the cost of introducing a bounded failure probability.

2.9 A cohomology-based algorithm for homology equivalence testing

Previously, our algorithms were primarily based on homology theory. In this section, we explore alternative solutions to the same problem using *cohomology theory*. Roughly speaking, homology theory builds upon simplices and the linear mappings between them (i.e., boundary maps). In contrast, cohomology theory

deals with linear functionals that assign real numbers to simplices. In this sense, cohomology can be viewed as a “dual” theory to homology (see Fig. 7).

A formal introduction to cohomology is provided in Section 6.1, but we briefly summarize the essential concepts relevant to our algorithm for testing homology equivalence:

- (i) An r -cochain is a linear functional that assigns a real value to any r -chain.
- (ii) The dual operator to the boundary map ∂_r is called the *coboundary map* δ^r .
- (iii) An r -cochain ω^r satisfying $\delta^r \omega^r = 0$ is called an r -cocycle.

Our cohomological algorithm is based on the following key property:

*If two cycles c_{r_1} and c_{r_2} are homologous, then $\omega^r(c_{r_1}) = \omega^r(c_{r_2})$ for all r -cocycles ω^r .
Otherwise, there exists some ω^r such that $\omega^r(c_{r_1}) \neq \omega^r(c_{r_2})$.*

We will provide a proof of this property in Section 6.1 and Section 6.2. Our quantum algorithm based on this idea is summarized in Algorithm 7. This leads to the following performance guarantee:

Theorem 2.6 (Time complexity of homology equivalence testing via cohomology, see Section 6.3). *Given a simplicial complex K with classical description $\{\mathcal{S}_r\}$, determining whether two given r -cycles c_{r_1}, c_{r_2} are homologous requires different resources depending on the construction method of the r -cocycle. If block encodings are constructed via projection onto $\ker(\delta_r)$, the quantum time complexity is $\mathcal{O}(r \log |\mathcal{S}_r|)$. Alternatively, in the manual construction via explicit representatives, the quantum time is $\mathcal{O}(\log |\mathcal{S}_r|)$, with an additional classical post-processing cost of $\mathcal{O}(r \log |\mathcal{S}_r|)$.*

In comparison, the homology-based approach to this problem has complexity

$$\mathcal{O}\left(\frac{\log(r|\mathcal{S}_{r+1}^K|) \log((r+2)|\mathcal{S}_{r+1}^K| + L)|\mathcal{S}_{r+1}^K|^2)}{(\text{rank}(\partial_{r+1}))^2}\right). \quad (2.26)$$

As discussed earlier, this homology-based method is effective only when $\text{rank}(\partial_{r+1})$ is large. On the other hand, the cohomological approach does not depend on such rank, and thus performs robustly regardless of the topological structure of the complex. This highlights the surprising power and generality of cohomology compared to homology in this context.

3 Preliminaries and related work

In this section, we provide a self-contained summary of the quantum algorithms and the mathematical background required for our approach.

3.1 Block-encoding and quantum singular value transformation

We introduce the main quantum ingredients required for the construction of our algorithm. For brevity, we recapitulate only the key results and omit technical details, which are thoroughly presented in [GSLW19].

Definition 3.1 (Block-encoding unitary, see e.g. [LC17, LC19, GSLW19]). *Let A be a Hermitian matrix of size $N \times N$ with operator norm $\|A\| < 1$. A unitary matrix U is said to be an exact block encoding of A if*

$$U = \begin{pmatrix} A & * \\ * & * \end{pmatrix}, \quad (3.1)$$

where the top-left block of U corresponds to A . Equivalently, one can write

$$U = |0\rangle\langle 0| \otimes A + (\dots), \quad (3.2)$$

where $|0\rangle$ denotes an ancillary state used for block encoding, and (\dots) represents the remaining components orthogonal to $|0\rangle\langle 0| \otimes A$. If instead U satisfies

$$U = |0\rangle\langle 0| \otimes \tilde{A} + (\dots), \quad (3.3)$$

for some \tilde{A} such that $\|\tilde{A} - A\| \leq \epsilon$, then U is called an ϵ -approximate block encoding of A . Furthermore, the action of U on a state $|0\rangle|\phi\rangle$ is given by

$$U |0\rangle|\phi\rangle = |0\rangle A |\phi\rangle + |\text{garbage}\rangle, \quad (3.4)$$

where $|\text{garbage}\rangle$ is a state orthogonal to $|0\rangle A |\phi\rangle$. The circuit complexity (e.g., depth) of U is referred to as the complexity of block encoding A .

Based on [Definition 3.1](#), several properties, though immediate, are of particular importance and are listed below.

Remark 3.1 (Properties of block-encoding unitary). *The block-encoding framework has the following immediate consequences:*

- (i) Any unitary U is trivially an exact block encoding of itself.
- (ii) If U is a block encoding of A , then so is $\mathbb{1}_m \otimes U$ for any $m \geq 1$.
- (iii) The identity matrix $\mathbb{1}_m$ can be trivially block encoded, for example, by $\sigma_z \otimes \mathbb{1}_m$.

Given a set of block-encoded operators, a variety of arithmetic operations can be performed on them. In the following, we present several operations that are particularly relevant and important to our algorithm. Here, we omit the proofs and focus on the implementation aspects, particularly the time complexity. Detailed discussions can be found, for instance, in [\[GSLW19, CVB20\]](#).

Lemma 3.1 (Informal, product of block-encoded operators, see e.g. [\[GSLW19\]](#)). *Given unitary block encodings of two matrices A_1 and A_2 , with respective implementation complexities T_1 and T_2 , there exists an efficient procedure for constructing a unitary block encoding of the product $A_1 A_2$ with complexity $T_1 + T_2$.*

Lemma 3.2 (Informal, tensor product of block-encoded operators, see e.g. [\[CVB20, Theorem 1\]](#)). *Given unitary block-encodings $\{U_i\}_{i=1}^m$ of multiple operators $\{M_i\}_{i=1}^m$ (assumed to be exact), there exists a procedure that constructs a unitary block-encoding of $\bigotimes_{i=1}^m M_i$ using a single application of each U_i and $\mathcal{O}(1)$ SWAP gates.*

Lemma 3.3 (Informal, linear combination of block-encoded operators, see e.g. [\[GSLW19, Theorem 52\]](#)). *Given the unitary block encoding of multiple operators $\{A_i\}_{i=1}^m$. Then, there is a procedure that produces a unitary block encoding operator of $\sum_{i=1}^m \pm(A_i/m)$ in time complexity $\mathcal{O}(m)$, e.g., using the block encoding of each operator A_i a single time.*

Lemma 3.4 (Informal, Scaling multiplication of block-encoded operators). *Given a block encoding of some matrix A , as in [Definition 3.1](#), the block encoding of A/p where $p > 1$ can be prepared with an extra $\mathcal{O}(1)$ cost.*

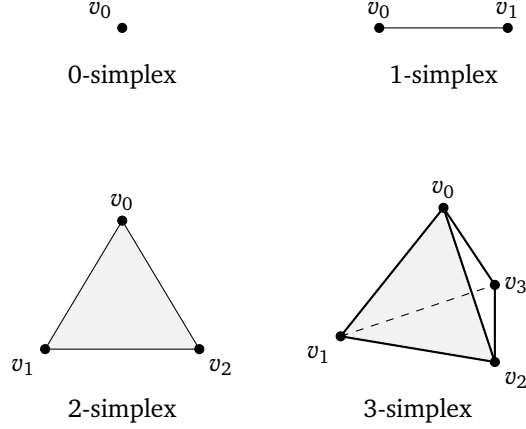


Figure 8: **Illustration of standard simplexes.** Top left: a point (0-simplex); top right: a line segment (1-simplex); bottom left: a filled triangle (2-simplex); bottom right: a filled tetrahedron (3-simplex). Each r -simplex is formed by $(r+1)$ -geometrically independent vertices in Euclidean space.

To show this, we note that the matrix representation of the R_Y rotation gate is given by

$$R_Y(\theta) = \begin{pmatrix} \cos(\theta/2) & -\sin(\theta/2) \\ \sin(\theta/2) & \cos(\theta/2) \end{pmatrix}. \quad (3.5)$$

If we choose $\theta = 2 \cos^{-1}(1/p)$, then by [Lemma 3.2](#), we can construct a block-encoding of $R_Y(\theta) \otimes \mathbb{1}_{\dim(A)}$, where $\dim(A)$ refers to the dimension of the rows (or columns) of the square matrix A . This operation results in a diagonal matrix of size $\dim(A) \times \dim(A)$ with all diagonal entries equal to $1/p$. Then, by applying [Lemma 3.1](#), we can construct a block-encoding of

$$(1/p) \mathbb{1}_{\dim(A)} \cdot A = A/p. \quad (3.6)$$

Lemma 3.5 (Matrix inversion, see e.g. [\[GSLW19, CKS17\]](#)). *Given a block encoding of some matrix A with operator norm $\|A\| \leq 1$ and block-encoding complexity T_A , then there is a quantum circuit producing an ϵ -approximated block encoding of A^{-1}/κ where κ is the conditional number of A . The complexity of this quantum circuit is $\mathcal{O}(\kappa T_A \log(1/\epsilon))$.*

3.2 Algebraic topology

This section provides a self-contained introduction to algebraic topology, with an emphasis on key concepts from homology theory and their application to the emerging field of topological data analysis. For a more comprehensive treatment, we refer the reader to standard texts such as [\[Hat05, Nak18\]](#).

We begin by introducing the discrete geometric objects known as *simplexes*. A simplex is a set of *geometrically independent* points. More precisely, a collection of $(r+1)$ points forms an r -simplex if no $(r-1)$ -dimensional affine subspace contains all of them. Let v_0, v_1, \dots, v_r be $r+1$ points in \mathbb{R}^m (with $m \geq r$); then the corresponding r -simplex is denoted by $\sigma_r = [v_0, v_1, \dots, v_r]$. The [Fig. 8](#) illustrates examples of simplexes of various dimensions.

Higher-order simplexes can be naturally generalized from the basic examples. Essentially, a simplex is a set of mutually connected, geometrically independent points. For instance, a 3-simplex $\sigma_3 = [v_0, v_1, v_2, v_3]$ contains several 2-simplex faces, such as $[v_0, v_1, v_2]$, $[v_0, v_2, v_3]$, $[v_1, v_2, v_3]$, and $[v_0, v_1, v_3]$. In general, an r -simplex has exactly $(r+1)$ faces, each of which is an $(r-1)$ -simplex obtained by omitting one of its vertices.

Remark 3.2 (Simplicial complex). *A simplicial complex K consists of simplexes arranged in a way that:*

- (i) *Every face of a simplex in the complex is itself part of the complex.*
- (ii) *The overlap of any two simplexes, if nonempty, must be a face common to both.*

As the next step, we define the chain group (or chain space) and the boundary map. For convenience, we denote S_r^K as the set of r -simplices in the simplicial complex K , i.e., $S_r^K := \{\sigma_{r_i}\}_{i=1}^{|S_r^K|}$. The r -th chain group, denoted C_r^K , is a free Abelian group finitely generated by all r -simplices. That is, an element $c_r \in C_r^K$, called an r -chain, has the form

$$c_r = \sum_{i=1}^{|S_r^K|} a_i \sigma_{r_i}, \quad (3.7)$$

where each coefficient a_i belongs to a coefficient ring, typically $\in \mathbb{Z}$ (integers), but may also be taken as $\in \mathbb{R}$ (real numbers), depending on the context.

A boundary map ∂_r is a group homomorphism $\partial_r : C_r^K \rightarrow C_{r-1}^K$, defined by its action on the basis elements. For an arbitrary r -simplex $\sigma_r = [v_0, v_1, \dots, v_r]$, the boundary map acts as

$$\partial_r [v_0, v_1, \dots, v_r] = \sum_{i=0}^r (-1)^i [v_0, \dots, \hat{v}_i, \dots, v_r], \quad (3.8)$$

where \hat{v}_i indicates that the vertex v_i is omitted. Intuitively, the boundary map ∂_r decomposes an r -simplex into a sum of its $(r-1)$ -dimensional faces. Its action on a general r -chain

$$c_r = \sum_{i=1}^{|S_r^K|} a_i \sigma_{r_i} \quad (3.9)$$

is extended linearly:

$$\partial_r c_r = \sum_{i=1}^{|S_r^K|} a_i \partial_r \sigma_{r_i}. \quad (3.10)$$

For an r -chain c_r , if $\partial_r c_r = 0$, then c_r is called an r -cycle. If there exist an $(r+1)$ -chain c_{r+1} such that $\partial_{r+1} c_{r+1} = c_r$, then c_r is called an r -boundary. A fundamental property of the boundary map is that $\partial_r \partial_{r+1} = 0$, i.e., the boundary of a boundary is zero (or “boundaryless”).

For the r -th chain group C_r^K , the set of all r -cycles forms the cycle group Z_r^K , and the set of all r -boundaries forms the boundary group B_r^K . Due to the identity $\partial_r \partial_{r+1} = 0$, every boundary is a cycle, and hence we have the inclusion $B_r^K \subseteq Z_r^K$. The r -th homology group is defined as the quotient group $H_r^K \equiv Z_r^K / B_r^K$. The rank of this group is called the r -th Betti number β_r , which counts the number of r -dimensional “holes” in the simplicial complex K . For example, a 1-dimensional hole corresponds to a loop, a 2-dimensional hole to a void, and so on. As a fundamental result in algebraic topology, Betti numbers are topological invariants. That is, they remain unchanged under homeomorphisms. By computing Betti numbers, one can classify and distinguish different topological spaces, each represented as a simplicial complex.

3.3 Topological data analysis

Topological Data Analysis (TDA) is an emerging direction in data science that applies concepts from algebraic topology, particularly homology theory, to the analysis of high-dimensional and large-scale data [Was16, Bub15]. A central motivation for TDA is that high-dimensional data often incur significant computational costs when processed by conventional techniques such as machine learning algorithms. In addition, such data may exhibit intricate geometric or topological structures that are not easily captured by traditional statistical or learning-based methods, but which naturally fall within the scope of algebraic topology. TDA provides a principled framework for extracting such structural information in a way that is both mathematically robust and computationally tractable.

A very practical problem in topological data analysis (TDA) is analyzing a point cloud to reveal its underlying “shape.” Suppose we are given n distinct points, each represented as an m -dimensional vector in \mathbb{R}^m . By imposing a metric, such as the Euclidean metric, we can define a distance between any pair of points. If the distance between two points is less than a chosen threshold $\bar{\epsilon}$, then we connect them by an edge. This results in a graph with n vertices and an associated connectivity structure. Each clique, meaning a fully connected subgraph, can be regarded as a simplex of the corresponding dimension. For example, a clique of $(r+1)$ vertices represents an r -simplex. In this way, we construct a simplicial complex K .

As mentioned earlier, Betti numbers, which are the ranks of homology groups, are topological invariants. Therefore, knowledge of these numbers at a given threshold $\bar{\epsilon}$ provides information about the shape of the point cloud. The parameter $\bar{\epsilon}$ is commonly referred to as the *length scale*. One of the main objectives of TDA is to understand the structure of a point cloud at various length scales. Betti numbers capture the number of topological features in the simplicial complex, such as connected components, loops, and voids. Features that emerge at a particular threshold $\bar{\epsilon}_1$ and disappear at another $\bar{\epsilon}_2$ are typically considered as noise. By examining how these features persist over different scales, TDA provides insight into the underlying structure of complex and potentially high-dimensional data.

Suppose that from a set of n data points in \mathbb{R}^m , equipped with a suitable metric and a chosen threshold $\bar{\epsilon}$, we construct a simplicial complex K . The primary objective is to analyze its topological structure, for instance, by estimating its Betti numbers. Since homology theory is inherently Abelian, the associated chain groups can be treated as vector spaces. This algebraic structure makes computation more tractable, as one can apply techniques from numerical linear algebra. For example, the r -th chain group is generated by the set of r -simplices $\{\sigma_{r_i}\}_{i=1}^{|\mathcal{S}_r^K|}$. We define the corresponding r -th chain vector space as the span of $\{|\sigma_{r_i}\rangle\}_{i=1}^{|\mathcal{S}_r^K|}$, where each $|\sigma_{r_i}\rangle$ serves as a basis vector. With a slight abuse of notation, we denote this vector space by C_r^K , referring to the r -chain space associated with the r th chain group. Its dimension is simply $|\mathcal{S}_r^K|$, the number of r -simplices in K .

The boundary map ∂_r is then a linear operator from C_r^K to C_{r-1}^K , and its matrix representation is determined with respect to the bases $\{|\sigma_{r_i}\rangle\}_{i=1}^{|\mathcal{S}_r^K|}$ for C_r^K and $\{|\sigma_{(r-1)_i}\rangle\}_{i=1}^{|\mathcal{S}_{r-1}^K|}$ for C_{r-1}^K . The action of ∂_r on any $|\sigma_{r_i}\rangle$ yields a linear combination of the vectors in the latter basis.

The homology group is defined as the quotient space $H_r^K = Z_r^K / B_r^K$, where Z_r^K is the cycle space and B_r^K is the boundary space. The computation of Betti numbers then reduces to finding the dimension of H_r^K . The so-called r -th combinatorial Laplacian is defined as in Eq. (2.1), and a standard result in the field gives $\dim \ker(\Delta_r) = \beta_r$. Therefore, the Betti number can be obtained by analyzing the spectrum of the combinatorial Laplacian. In practice, this can be done classically by applying Gaussian elimination to find the dimension of the kernel of Δ_r , which yields the desired Betti number. The time complexity of this classical algorithm is $\mathcal{O}(|\mathcal{S}_r^K|^3)$ [Was16].

Quantum algorithms for estimating Betti numbers β_r (for all r) were first proposed in the work of Lloyd, Garnerone, and Zanardi [LGZ16], often referred to as the LGZ algorithm. The main ideas behind

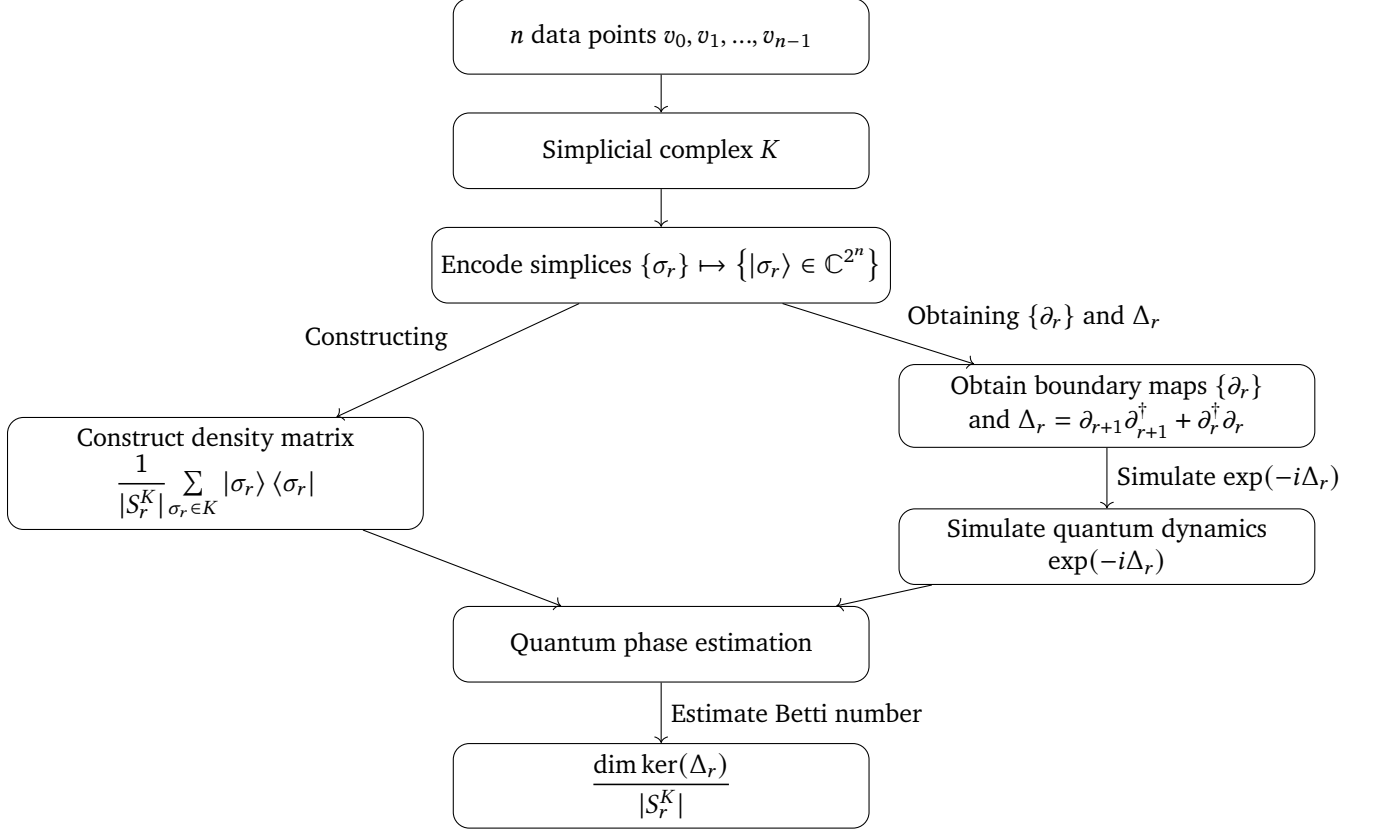


Figure 9: **Quantum algorithm for estimating Betti numbers (LGZ algorithm)**. The procedure begins with n data points, from which a simplicial complex K is constructed. Each r -simplex $\sigma_r \in K$ is encoded into an n -qubit basis state $|\sigma_r\rangle$. A uniform mixture over all such basis states yields a density matrix, while the combinatorial Laplacian Δ_r is computed using the boundary maps. Quantum dynamics governed by $\exp(-i\Delta_r)$ is simulated, and quantum phase estimation is used to estimate the fraction of zero eigenvalues of Δ_r , which corresponds to the normalized r -th Betti number.

the LGZ algorithm are as follows.

Given a simplicial complex K constructed from a set of n points, labeled v_0, v_1, \dots, v_{n-1} , the algorithm encodes simplices into the computational basis states of an n -qubit quantum system. Each r -simplex σ_r is represented as a quantum binary string $|\sigma_r\rangle \in \mathbb{C}^{2^n}$ with Hamming weight $(r+1)$. The positions of the ones in this string correspond to the vertices included in the simplex. In this encoding, each chain group of K corresponds to a subspace of the n -qubit Hilbert space \mathbb{C}^{2^n} . The algorithm assumes access to a membership oracle, which determines whether a given r -simplex σ_r belongs to the complex K . This oracle acts as

$$O_r^K |\sigma_{r_i}\rangle |0\rangle = |\sigma_{r_i}\rangle |0 \text{ or } 1\rangle, \quad (3.11)$$

where the second register is 1 if and only if $\sigma_r \in K$. Given this encoding and access to the oracle, the LGZ algorithm proceeds with a quantum procedure for estimating the Betti numbers, as summarized in Fig. 9.

The output of the LGZ algorithm described above is an estimate of the quantity $\dim \ker(\Delta_r)/|S_r^K|$, commonly referred to as the normalized r -th Betti number. Following its introduction, several subsequent works have refined and analyzed this algorithm further [US16, BSG⁺24, MGB22, SL23, Hay22]. We refer the interested reader to these references for a more comprehensive treatment. In this section, we highlight two key aspects that motivate the present work:

- (i) It has been shown in [SL23] that computing Betti numbers exactly is #P-hard, and estimating them is NP-hard, even for a simplicial complex specified via a standard oracle access model.
- (ii) To the best of our knowledge, the most efficient quantum complexities known for approximating normalized Betti numbers to additive error ϵ and unnormalized Betti numbers to multiplicative error δ are given by:

$$\mathcal{O}\left(\frac{1}{\epsilon} \cdot \left(n^2 \sqrt{\frac{\binom{n}{r+1}}{|S_r^K|}} + n\kappa\right)\right), \quad \mathcal{O}\left(\frac{1}{\delta} \cdot \left(n^2 \sqrt{\frac{\binom{n}{r+1}}{\beta_r}} + n\kappa \sqrt{\frac{|S_r^K|}{\beta_r}}\right)\right), \quad (3.12)$$

where κ denotes the condition number of the Laplacian Δ_r .

These two results, while ostensibly distinct, are in fact complementary. The former indicates a fundamental computational hardness barrier, suggesting that exponential quantum speed-ups are unlikely for general instances of the problem. The latter characterizes the regime in which quantum advantage may be possible, namely when the Betti number β_r is close to the total number of r -simplices, $|S_r^K|$, and when $|S_r^K|$ itself approaches the combinatorial upper bound $\binom{n}{r+1}$. This is sometimes referred to as the simplex-dense regime. However, as noted in [SL23, BSG⁺24], complexes satisfying both conditions: large β_r and simplex-dense structure, are rare in practical settings. As such, the question of whether quantum algorithms can yield a meaningful advantage in topological data analysis remains largely open.

Motivated by this, we delve deeper into the algorithmic structure of the LGZ approach. It seems counterintuitive that quantum advantage arises predominantly in the simplex-dense regime. This behavior stems from a key technical step: constructing the uniform mixture

$$\frac{1}{|S_r^K|} \sum_{\sigma_r \in K} |\sigma_r\rangle \langle \sigma_r| \quad (3.13)$$

via a multi-solution variant of Grover's algorithm, using the membership oracle O_r^K . The associated query complexity scales as

$$\mathcal{O}\left(\sqrt{\frac{\binom{n}{r+1}}{|S_r^K|}}\right), \quad (3.14)$$

which becomes expensive in the simplex-sparse regime, i.e., when $|S_r^K| \ll \binom{n}{r+1}$.

From a classical standpoint, this is at odds with intuition. One expects the complexity of estimating Betti numbers to grow with the number of simplices, as this reflects the dimensionality of the chain groups. Indeed, a recent approach based on quantum cohomology [NGW23] has demonstrated better performance in the simplex-sparse regime, aligning more closely with classical heuristics. This observation motivates the conjecture that homology-based quantum algorithms should similarly exhibit optimal behavior in sparse settings.

Furthermore, [SL23] emphasized that a meaningful quantum speed-up is unlikely when the input is given in the most generic form—that is, merely as a list of vertices and pairwise connections—since the simplicial complex must then be constructed algorithmically, incurring the full cost of oracle queries and Grover search. Instead, the complex must be specified in more detail to avoid this bottleneck. An illustrative example provided therein involves a dataset of Facebook users, where higher-order relationships (e.g., groups of friends) are explicitly known.

In the following, we build upon the insight articulated in [SL23], namely that an explicit specification of the simplicial complex is necessary in order to achieve quantum speed-up. As we demonstrate in the

next section, when such a specification is provided, quantum algorithms can estimate (normalized) Betti numbers with exponential speed-up over known classical approaches. Moreover, the regime in which this advantage is most pronounced corresponds to the simplex-sparse setting, aligning with classical complexity expectations.

Finally, one of the key subroutines in our quantum algorithm involves stochastic rank estimation. The time complexity of this procedure is given as follows, and the detailed algorithm is presented in [Appendix B](#).

Lemma 3.6 (Stochastic rank estimation, see e.g. [US16, USS17, UAS⁺21]). *Let H be an $N \times N$ Hermitian matrix with minimum eigenvalue $\lambda_{\min}(H)$. Then, the ratio $\text{rank}(H)/N$ can be estimated to additive accuracy ϵ in time complexity*

$$\mathcal{O}\left(\frac{1}{\epsilon^2} \log\left(\frac{1}{\lambda_{\min}(H)}\right)\right). \quad (3.15)$$

4 Alternative quantum algorithm for estimating Betti numbers

4.1 Simplicial complex specification

Our approach remains grounded in homology theory, with the central computational task being the determination of the dimension of the kernel of the combinatorial Laplacian Δ_r . The first step, therefore, is to specify and provide access to the simplicial complex K of interest. Recall that S_r^K denotes the set of r -simplices in K , where K is a simplicial complex over a set of n vertices.

Rather than encoding simplices as binary strings with appropriate Hamming weight, we instead index them using integers. Specifically, we label the elements of S_r^K as $[[S_r^K]] := \{1, 2, \dots, |S_r^K|\}$ for each $r \in \{1, 2, \dots, n\}$. The specification of K is then defined to be classical knowledge of all simplices and their face relationships. That is, for any r -simplex σ_{r_i} and any $(r-1)$ -simplex $\sigma_{(r-1)_j}$, the specification includes knowledge of whether $\sigma_{(r-1)_j} \subseteq \sigma_{r_i}$, for all $i \in [[S_r^K]]$ and $j \in [[S_{r-1}^K]]$.

This setup mirrors that of the classical setting described earlier in [Section 3.3](#). To make this concrete, suppose we begin with n data points v_0, v_1, \dots, v_{n-1} . In principle, any subset of $(r+1)$ points may form a potential r -simplex. Out of all $\binom{n}{r+1}$ possible r -simplices, we select a subset of size $|S_r^K|$ and assign them integer labels from 1 to $|S_r^K|$. Each r -simplex σ_{r_i} consists of $(r+1)$ distinct $(r-1)$ -faces. For each such simplex, we identify the corresponding $(r-1)$ -simplices from S_{r-1}^K that constitute its boundary. We represent this structure via a matrix

$$\mathcal{S}_r \in \{0, 1\}^{|S_{r-1}^K| \times |S_r^K|}, \quad (4.1)$$

where the (j, i) -th entry is 1 if $\sigma_{(r-1)_j}$ is a face of σ_{r_i} , and 0 otherwise. Since any two distinct r -simplices share at most one common $(r-1)$ -face, any two columns of \mathcal{S}_r have at most one overlapping nonzero entry. This construction is repeated for all $r = 1, 2, \dots, n$, and provides a compact, face-based specification of the simplicial complex K .

To illustrate the above procedure, we consider a set of five data points: $\{v_i\}_{i=0}^4$. We define the set of 2-simplices as

$$S_2^K = \{[v_0, v_1, v_2], [v_0, v_3, v_4], [v_1, v_2, v_3]\},$$

and assign them labels 1, 2, 3, respectively. The set of 1-simplices is given by

$$S_1^K = \{[v_0, v_1], [v_0, v_2], [v_1, v_2], [v_0, v_3], [v_3, v_4], [v_0, v_4], [v_1, v_3], [v_2, v_3], [v_2, v_4]\},$$

which we label as 1 through 9 in the order listed.

Using this labeling, we construct the matrix $\mathcal{S}_2 \in \{0, 1\}^{9 \times 3}$ that encodes the face relationships between 1- and 2-simplices. Each column corresponds to a 2-simplex, and each row corresponds to a 1-simplex. The (i, j) -th entry is 1 if the i -th 1-simplex is a face of the j -th 2-simplex, and 0 otherwise. The resulting matrix is:

$$\mathcal{S}_2 = \begin{pmatrix} 1 & 1 & 1 & 0 & 0 & 0 & 0 & 0 & 0 \\ 0 & 0 & 0 & 1 & 1 & 1 & 0 & 0 & 0 \\ 0 & 0 & 1 & 0 & 0 & 0 & 1 & 1 & 0 \end{pmatrix}^T \quad (4.2)$$

A similar labeling procedure can be applied to define \mathcal{S}_1 for the face relations between 0- and 1-simplices. We remark that the topological structure of the simplicial complex K is invariant under the labeling of its simplices. Hence, the specification described above is without loss of generality. Indeed, in classical settings, simplicial complexes are typically specified in this way, by explicitly listing simplices and their inclusion relations.

4.2 Estimating (normalized) Betti numbers

This classical specification $\{\mathcal{S}_r\}$ allows us to explicitly construct the matrix representation of the boundary map ∂_r , which is a matrix of size $|S_{r-1}^K| \times |S_r^K|$. Given such a matrix, we can leverage the following result:

Lemma 4.1 (Entry-computable block-encoding of sparse matrices, see e.g. [Ngh25]). *Let A be an $M \times N$ matrix with classically known entries and Frobenius norm $\|A\|_F$. Then there exists a quantum circuit of depth $\mathcal{O}(\log(sN))$ that implements a block-encoding of $A^\dagger A / \|A\|_F^2$, using $\mathcal{O}(Ns)$ ancilla qubits, where s is the sparsity of A .¹*

In our setting, each column of ∂_r contains exactly $(r+1)$ nonzero entries, each equal to 1. Consequently, the Frobenius norm of ∂_r is given by

$$\|\partial_r\|_F = ((r+1)|S_r^K|)^{1/2}. \quad (4.3)$$

Applying Lemma 4.1 to ∂_r , we obtain a block-encoding of the normalized matrix

$$\frac{\partial_r^\dagger \partial_r}{(r+1)|S_r^K|}. \quad (4.4)$$

Analogously, applying the same construction to ∂_{r+1} yields a block-encoding of

$$\frac{\partial_{r+1}^\dagger \partial_{r+1}}{(r+2)|S_{r+1}^K|}. \quad (4.5)$$

Our next objective is to construct a block-encoding of Δ_r , up to a proportional constant. To this end, we apply Lemma 3.4 to rescale the previously obtained block-encoded operators Eq. (4.4) and Eq. (4.5) as follows. First, applying the lemma to the block-encoding in Eq. (4.4), we obtain the normalized operator

$$\frac{\partial_r^\dagger \partial_r}{(r+1)(r+2)|S_r^K||S_{r+1}^K|}. \quad (4.6)$$

¹We remark a subtlety. The method in [Ngh25] employs the state preparation technique in [ZLY22]. In fact, this preparation step requires a classical pre-processing of complexity $\mathcal{O}(\log N)$. However, such complexity can be reduced to $\mathcal{O}(1)$ if the matrix A is mainly composed of similar entries. In that case, the output of a classical pre-processing step can be applied to many entries. In this work, the boundary operator ∂_r has entries to be either 1 or -1 , and thus the classical pre-processing cost is very modest, negligible.

Similarly, applying the same rescaling to Eq. (4.5) yields

$$\frac{\partial_{r+1} \partial_{r+1}^\dagger}{(r+1)(r+2)|S_r^K||S_{r+1}^K|}. \quad (4.7)$$

We then apply Lemma 3.3 to obtain a block-encoding of their sum:

$$\frac{\Delta_r}{2(r+1)(r+2)|S_r^K||S_{r+1}^K|}. \quad (4.8)$$

The final step is to estimate the dimension of the kernel of Δ_r . In principle, several approaches are available for this task. For instance, one may use quantum phase estimation, akin to the LGZ algorithm, or employ the block measurement technique introduced in [Hay22]. Both methods incur a complexity that is polynomial in the inverse of the spectral gap (the difference between the zero eigenvalue and the smallest nonzero eigenvalue) and linear in the inverse of the desired precision. In our case, the spectral gap of the above-normalized operator is approximately $\sim (2(r+1)(r+2)|S_r^K||S_{r+1}^K|)^{-1}$, implying that the inverse gap scales as $\mathcal{O}(r^2|S_r^K||S_{r+1}^K|)$.

Such a scaling leads to substantial computational overhead. A more efficient alternative is the stochastic rank estimation method proposed in [UAS⁺21] (see also Lemma 3.6), which achieves complexity logarithmic in the inverse of the spectral gap, an exponential improvement over the aforementioned techniques, at the cost of being quadratically slower in the inverse of the precision. A summary of this method is provided in the Appendix B. To analyze the overall complexity, we summarize the key steps involved in the construction.

- (i) **Block-encoding of boundary operators:** We first apply Lemma 4.1 to construct block-encodings of

$$\frac{\partial_i^\dagger \partial_i}{(i+1)|S_i^K|} \quad (4.9)$$

and their transposes for $i = r, r+1$. According to Lemma 4.1, as the matrix ∂_r is of size $|S_{r-1}^K| \times |S_r^K|$ and sparsity $r+1$, this step has complexity $\mathcal{O}(\log(r|S_r^K|))$.

- (ii) **Rescaling of block-encoded operators:** Using Lemma 3.4, we obtain the rescaled block-encoding of Eq. (4.6) from Eq. (4.4). This involves one invocation of the block-encoding and one additional single-qubit gate. The complexity remains $\mathcal{O}(\log(r|S_r^K|))$.
- (iii) **Summation of rescaled operators:** By Lemma 3.3, we construct the block-encoding of the operator Eq. (4.8), using the block-encodings Eq. (4.6) and Eq. (4.7) once each. The resulting complexity is again $\mathcal{O}(\log(r|S_r^K|))$.
- (iv) **Stochastic rank estimation:** Finally, we employ the stochastic rank estimation method of [UAS⁺21] to approximate the normalized rank $\text{rank}(\Delta_r)/|S_r^K|$, from which the normalized kernel dimension follows as

$$\frac{\dim \ker(\Delta_r)}{|S_r^K|} = 1 - \frac{\text{rank}(\Delta_r)}{|S_r^K|}. \quad (4.10)$$

The complexity of this estimation up to an additive error ϵ is the product of the complexity of preparing the block encoding in Eq. (4.8) and the complexity of estimating the above ratio via stochastic rank estimation, essentially applying Lemma 3.6 with accuracy ϵ and

$$\lambda_{\min}(H) \sim \frac{1}{2(r+1)(r+2)|S_r^K||S_{r+1}^K|}. \quad (4.11)$$

Therefore, the total complexity is:

$$\mathcal{O}\left(\frac{\log(r|S_r^K|) \log(r^2|S_r^K||S_{r+1}^K|)}{\epsilon^2}\right). \quad (4.12)$$

We remark that the outcome of the above procedure is an estimate of the quantity

$$1 - \frac{\text{rank}(\Delta_r)}{|S_r^K|} = \frac{\beta_r}{|S_r^K|}, \quad (4.13)$$

which is referred to as the normalized r -th Betti number. To estimate the (unnormalized) r -th Betti number β_r to multiplicative accuracy δ , it suffices to estimate the normalized Betti number to additive error

$$\epsilon = \delta \cdot \frac{\beta_r}{|S_r^K|}. \quad (4.14)$$

Substituting this value into the complexity bound of the stochastic rank estimation, we obtain the total complexity

$$\mathcal{O}\left(\frac{\log(r|S_r^K|) \log(r^2|S_r^K||S_{r+1}^K|)|S_r^K|^2}{\delta^2 \beta_r^2}\right). \quad (4.15)$$

4.3 Estimating (normalized) persistent Betti numbers

We now extend our discussion to the estimation of *persistent Betti numbers*, which generalize ordinary Betti numbers. In typical applications of TDA, the connectivity between data points is governed by a scale parameter $\bar{\epsilon}$. For a fixed threshold $\bar{\epsilon}$, one constructs a simplicial complex whose Betti numbers quantify the number of topological features such as connected components, loops, and voids. Specifically, the r -th Betti number counts the number of r -dimensional holes: for instance, the first Betti number measures the number of one-dimensional loops, and the second Betti number corresponds to the number of two-dimensional voids.

As the scale parameter increases from $\bar{\epsilon}_1$ to $\bar{\epsilon}_2$ with $\bar{\epsilon}_2 \geq \bar{\epsilon}_1$, additional simplices are added, yielding a new simplicial complex that is generally denser and topologically distinct from the former. The task then becomes identifying the topological features that persist across this range of scales. Persistent Betti numbers precisely quantify the number of such features that survive from the first complex to the second.

Quantum algorithms for estimating Betti numbers in this persistent setting were proposed in [Hay22] and [MGB22], under the assumption of oracle access to pairwise connectivity information at two different scales. In contrast, our approach assumes that classical descriptions of the simplicial complexes are available. Specifically, let K_1 and K_2 be two simplicial complexes with $K_1 \subseteq K_2$, meaning that every simplex in K_1 is also present in K_2 . Let $\{S_r^1\}$ and $\{S_r^2\}$ denote the sets of specification matrices associated with K_1 and K_2 , respectively, as defined in Section 4.1.

Given these classical specifications, we can apply the previously described procedures to construct block-encodings of the normalized combinatorial Laplacians

$$\frac{\Delta_r^{K_1}}{2(r+1)(r+2)|S_r^{K_1}||S_{r+1}^{K_1}|} \quad (4.16)$$

and

$$\frac{\Delta_r^{K_2}}{2(r+1)(r+2)|S_r^{K_2}||S_{r+1}^{K_2}|}. \quad (4.17)$$

These constructions form the foundation for the estimation of persistent Betti numbers in the presence of explicitly known simplicial complexes.

We now turn to the estimation of persistent Betti numbers, which generalize the notion of Betti numbers by capturing topological features that persist across a range of length scales in a filtration of simplicial complexes. Let $K_1 \subseteq K_2$ be two simplicial complexes, corresponding to two length scales $\bar{\epsilon}_1 \leq \bar{\epsilon}_2$ in the context of topological data analysis. For each $r \geq 0$, denote by $\Delta_r^{K_1}$ and $\Delta_r^{K_2}$ the r -th combinatorial Laplacians of K_1 and K_2 , respectively, which are square matrices of size $|S_r^{K_1}| \times |S_r^{K_1}|$ and $|S_r^{K_2}| \times |S_r^{K_2}|$. Since $K_1 \subseteq K_2$, it follows that $S_r^{K_1} \subseteq S_r^{K_2}$ and thus $|S_r^{K_1}| \leq |S_r^{K_2}|$ for all r .

Although the quantum algorithm previously described can be employed to estimate the normalized r -th Betti numbers of K_1 and K_2 individually, as observed in [Hay22], the difference between these two values does not, in general, yield the r -th persistent Betti number. To accurately compute the latter, a more refined construction is required, and we draw on the formalism developed in [Hay22], which we now summarize.

Let $\{\partial_r^{K_1}\}, \{\partial_r^{K_2}\}$ be the boundary maps associated with K_1 and K_2 , respectively. Because $K_1 \subseteq K_2$, the domain of $\partial_r^{K_1}$ is naturally a subspace of the domain of $\partial_r^{K_2}$ for each r . The r -th persistent homology group is defined as

$$H_r^{K_1, K_2} = \frac{\ker(\partial_r^{K_1})}{\text{im}(\partial_r^{K_2}) \cap \ker(\partial_r^{K_1})}, \quad (4.18)$$

and the corresponding r -th persistent Betti number is given by the rank of this quotient space.

To proceed, recall that the r -th chain group C_r^K is the vector space spanned by the r -simplices of K . The boundary operator ∂_r^K acts linearly from C_r^K to C_{r-1}^K . Given two complexes $K_1 \subseteq K_2$, we define the subspace $C_r^{K_1, K_2} := \{c \in C_r^{K_2} : \partial_r^{K_2}(c) \in C_{r-1}^{K_1}\} \subseteq C_r^{K_2}$, which consists of r -chains in K_2 whose boundaries lie in K_1 . Define $\partial_r^{K_1, K_2}$ as the restriction of $\partial_r^{K_2}$ to the domain $C_r^{K_1, K_2}$. This operator maps $C_r^{K_1, K_2}$ to $C_{r-1}^{K_1}$ by construction. Using this, we define the r -th *persistent combinatorial Laplacian* as

$$\Delta_r^{K_1, K_2} := \partial_{r+1}^{K_1, K_2} (\partial_{r+1}^{K_1, K_2})^\dagger + (\partial_r^{K_1})^\dagger \partial_r^{K_1}. \quad (4.19)$$

As shown in [Lim20], the dimension of the kernel of this operator precisely equals the r -th persistent Betti number.

Therefore, our goal reduces to constructing a block-encoding of $\Delta_r^{K_1, K_2}$. Among its two summands, the second term $(\partial_r^{K_1})^\dagger \partial_r^{K_1}$ can be efficiently block-encoded using the techniques established in the Section 3.1. The main challenge lies in constructing a block-encoding of the first term, $\partial_{r+1}^{K_1, K_2} (\partial_{r+1}^{K_1, K_2})^\dagger$, from the classical descriptions of K_1 and K_2 .

To construct the operator $\partial_{r+1}^{K_1, K_2} (\partial_{r+1}^{K_1, K_2})^\dagger$, we draw upon the machinery of the *Schur complement*, which plays a crucial role in isolating the effect of submatrices. Let $M \in \mathbb{R}^{N \times N}$ be a real square matrix. For subsets $I, J \subseteq [N] := \{1, 2, \dots, N\}$, let $M(I, J)$ denote the submatrix of M formed by rows indexed by I and columns indexed by J . The Schur complement of the principal submatrix $M(I, I)$ in M is defined by

$$M/M(I, I) := M(\bar{I}, \bar{I}) - M(\bar{I}, I)M(I, I)^+M(I, \bar{I}), \quad (4.20)$$

where $\bar{I} := [N] \setminus I$ and $M(I, I)^+$ denotes the Moore-Penrose pseudoinverse of $M(I, I)$.

Returning to our setting, recall that $S_r^{K_1}$ and $S_r^{K_2}$ are the sets of r -simplices of the simplicial complexes K_1 and K_2 , respectively, with $S_r^{K_1} \subseteq S_r^{K_2}$. Denote the integer set $[|S_r^{K_1}|] := \{1, 2, \dots, |S_r^{K_1}|\}$. Define the index set $I_{K_1}^{K_2} := [|S_r^{K_2}|] \setminus [|S_r^{K_1}|]$, which identifies the coordinates in $S_r^{K_2}$ not present in $S_r^{K_1}$. As established in Hodge theory [Lim20], the operator $\partial_{r+1}^{K_1, K_2} (\partial_{r+1}^{K_1, K_2})^\dagger$ can be expressed as a Schur complement of the

$$\partial_{r+1}^{K_2} = \begin{bmatrix} \mathcal{B} & \mathcal{R} \\ 0 & \mathcal{G} \\ 0 & \\ 0 & \end{bmatrix} \quad \text{and} \quad (\partial_{r+1}^{K_2})^\dagger = \begin{bmatrix} \mathcal{B}^\dagger & 0 & 0 & 0 \\ \mathcal{R}^\dagger & \mathcal{G}^\dagger \\ * & * & * \\ * & * & * \\ * & * & * \end{bmatrix}$$

Figure 10: **Block structure of the boundary matrix $\partial_{r+1}^{K_2}$ and its adjoint $(\partial_{r+1}^{K_2})^\dagger$.** The blue block \mathcal{B} corresponds to the original boundary operator $\partial_{r+1}^{K_1}$, while the red block \mathcal{R} represents the interaction between simplices in K_1 and those newly added in $K_2 \setminus K_1$. The green block \mathcal{G} encodes the internal structure among new simplices. Dashed outlines in the adjoint matrix highlight the transpose-like dual roles of each sub-block.

full operator $\partial_{r+1}^{K_2} (\partial_{r+1}^{K_2})^\dagger$, restricted to the relevant subspace. Explicitly, we have

$$\partial_{r+1}^{K_1, K_2} (\partial_{r+1}^{K_1, K_2})^\dagger = (\partial_{r+1}^{K_2} (\partial_{r+1}^{K_2})^\dagger) / (\partial_{r+1}^{K_2} (\partial_{r+1}^{K_2})^\dagger (I_{K_1}^{K_2}, I_{K_1}^{K_2})) \quad (4.21)$$

$$= \partial_{r+1}^{K_2} (\partial_{r+1}^{K_2})^\dagger (\bar{I}, \bar{I}) - \partial_{r+1}^{K_2} (\partial_{r+1}^{K_2})^\dagger (\bar{I}, I) (\partial_{r+1}^{K_2} (\partial_{r+1}^{K_2})^\dagger (I, I)) + \partial_{r+1}^{K_2} (\partial_{r+1}^{K_2})^\dagger (I, \bar{I}), \quad (4.22)$$

where $I := I_{K_1}^{K_2}$ and $\bar{I} := [S_r^{K_2}] \setminus I$. This formulation allows us to compute the persistent Laplacian using only the combinatorial Laplacian of K_2 , along with access to the inclusion structure between K_1 and K_2 . Importantly, it shows that $\partial_{r+1}^{K_1, K_2} (\partial_{r+1}^{K_1, K_2})^\dagger$ can be obtained as a Schur complement of the full Laplacian, thereby facilitating its block-encoding by quantum means, assuming access to a block-encoding of $\partial_{r+1}^{K_2} (\partial_{r+1}^{K_2})^\dagger$.

We now examine the structure of the boundary matrix $\partial_{r+1}^{K_2}$ in greater detail. Recall that this matrix represents the boundary operator $\partial_{r+1}^{K_2} : C_{r+1}^{K_2} \rightarrow C_r^{K_2}$, and hence it has dimensions $|S_r^{K_2}| \times |S_{r+1}^{K_2}|$. Given the inclusion of simplices, namely $S_{r+1}^{K_1} \subseteq S_{r+1}^{K_2}$ and $S_r^{K_1} \subseteq S_r^{K_2}$, it follows that the matrix $\partial_{r+1}^{K_2}$ contains the matrix $\partial_{r+1}^{K_1}$ as a submatrix in the top-left corner (see Fig. 10, left).

We now characterize the block structure of $\partial_{r+1}^{K_2}$. The blue block, denoted by \mathcal{B} , corresponds precisely to $\partial_{r+1}^{K_1}$ and has dimensions

$$\dim(\mathcal{B}) = |S_r^{K_1}| \times |S_{r+1}^{K_1}|. \quad (4.23)$$

The red block, denoted by \mathcal{R} , consists of the columns indexed by the new $(r+1)$ -simplices in K_2 (i.e., those in $S_{r+1}^{K_2} \setminus S_{r+1}^{K_1}$), and rows indexed by those r -simplices in K_1 which are faces of these new simplices. Thus, its dimension is given by

$$\dim(\mathcal{R}) = |S_r^{K_1}| \times (|S_{r+1}^{K_2}| - |S_{r+1}^{K_1}|). \quad (4.24)$$

Finally, the green block, denoted by \mathcal{G} , represents the portion of $\partial_{r+1}^{K_2}$ corresponding to both new rows and new columns, i.e., contributions from r -simplices in $S_r^{K_2} \setminus S_r^{K_1}$ and $(r+1)$ -simplices in $S_{r+1}^{K_2} \setminus S_{r+1}^{K_1}$. Therefore, its size is

$$\dim(\mathcal{G}) = (|S_r^{K_2}| - |S_r^{K_1}|) \times (|S_{r+1}^{K_2}| - |S_{r+1}^{K_1}|). \quad (4.25)$$

This block decomposition offers a clear perspective on how the boundary matrix of a filtered complex grows with the inclusion of new simplices, and will be fundamental in the forthcoming analysis. The matrix representation of the operator $(\partial_{r+1}^{K_2})^\dagger$ is shown in Fig. 10 (right), and it contains the conjugate transpose blocks \mathcal{B}^\dagger , \mathcal{R}^\dagger , and \mathcal{G}^\dagger .

We now examine the matrix product $\partial_{r+1}^{K_2} (\partial_{r+1}^{K_2})^\dagger$, which is of size $|S_r^{K_2}| \times |S_r^{K_2}|$. Define the index set $I_{K_1}^{K_2} := [|S_r^{K_2}|] / [|S_r^{K_1}|]$, representing the positions of the r -simplices in K_1 within K_2 . The submatrix $\partial_{r+1}^{K_2} (\partial_{r+1}^{K_2})^\dagger (I_{K_1}^{K_2}, I_{K_1}^{K_2})$ selects rows and columns indexed by $I_{K_1}^{K_2}$, and corresponds to the product $\mathcal{G}\mathcal{G}^\dagger$, i.e., the green block times its Hermitian transpose.

Next, consider the off-diagonal submatrix $\partial_{r+1}^{K_2} (\partial_{r+1}^{K_2})^\dagger ([|S_r^{K_2}|] \setminus I_{K_1}^{K_2}, I_{K_1}^{K_2})$, where the index set $[|S_r^{K_2}|] \setminus I_{K_1}^{K_2}$ corresponds to simplices originally in K_1 . This block captures interactions between rows from \mathcal{R} and columns from \mathcal{G}^\dagger , hence equals $\mathcal{R}\mathcal{G}^\dagger$. Similarly, the conjugate transpose of this block, $\partial_{r+1}^{K_2} (\partial_{r+1}^{K_2})^\dagger (I_{K_1}^{K_2}, [|S_r^{K_2}|] \setminus I_{K_1}^{K_2})$, is given by $\mathcal{G}\mathcal{R}^\dagger$. The remaining principal block, $\partial_{r+1}^{K_2} (\partial_{r+1}^{K_2})^\dagger ([|S_r^{K_2}|] \setminus I_{K_1}^{K_2}, [|S_r^{K_2}|] \setminus I_{K_1}^{K_2})$, represents the contribution from both \mathcal{B} and \mathcal{R} , and is thus equal to the sum $\mathcal{B}\mathcal{B}^\dagger + \mathcal{R}\mathcal{R}^\dagger$.

Combining all parts and applying the Schur complement (cf. Eq. (4.21)), we obtain the expression:

$$\partial_{r+1}^{K_1, K_2} (\partial_{r+1}^{K_1, K_2})^\dagger = \mathcal{B}\mathcal{B}^\dagger + \mathcal{R}\mathcal{R}^\dagger - \mathcal{R}\mathcal{G}^\dagger (\mathcal{G}\mathcal{G}^\dagger)^+ \mathcal{G}\mathcal{R}^\dagger, \quad (4.26)$$

where $(\mathcal{G}\mathcal{G}^\dagger)^+$ denotes the Moore–Penrose pseudoinverse. Since $\mathcal{G}\mathcal{G}^\dagger$ is square and Hermitian, its pseudoinverse coincides with the standard matrix inverse: $(\mathcal{G}\mathcal{G}^\dagger)^+ = (\mathcal{G}\mathcal{G}^\dagger)^{-1}$.

Now, let us return to the matrix representation of $\partial_{r+1}^{K_2}$. Given a classical description of K_2 , the matrix $\partial_{r+1}^{K_2}$ is fully determined, and consequently, all the block matrices \mathcal{B} , \mathcal{R} , and \mathcal{G} are explicitly known. Therefore, by invoking Lemma 4.1, we can construct the block encodings of the following normalized operators: $\mathcal{B}\mathcal{B}^\dagger / \|\mathcal{B}\|_F^2$, $\mathcal{G}\mathcal{G}^\dagger / \|\mathcal{G}\|_F^2$, and $\mathcal{R}\mathcal{R}^\dagger / \|\mathcal{R}\|_F^2$. To advance further, we introduce the following essential result:

Lemma 4.2 (Positive power of a positive matrix, see e.g. [GSLW19]). *Let \mathcal{M} be a positive matrix with a block encoding, satisfying:*

$$\frac{\mathbb{1}}{\kappa_M} \leq \mathcal{M} \leq \mathbb{1}. \quad (4.27)$$

Then for any $c \in (0, 1)$, one can implement an ϵ -approximate block encoding of $\mathcal{M}^c / 2$ with time complexity $\mathcal{O}(\kappa_M T_M \log^2(\kappa_M / \epsilon))$, where T_M denotes the complexity of the block encoding of \mathcal{M} .

Utilizing this lemma, we obtain the following transformations on the block-encoded operators:

$$\frac{\mathcal{R}\mathcal{R}^\dagger}{\|\mathcal{R}\|_F^2} \rightarrow \frac{\mathcal{R}^\dagger}{\|\mathcal{R}\|_F}, \quad \frac{\mathcal{G}\mathcal{G}^\dagger}{\|\mathcal{G}\|_F^2} \rightarrow \frac{\mathcal{G}^\dagger}{\|\mathcal{G}\|_F}. \quad (4.28)$$

Moreover, Lemma 3.5 allows us to realize the inverse transformation:

$$\frac{\mathcal{G}\mathcal{G}^\dagger}{\|\mathcal{G}\|_F^2} \rightarrow \frac{1}{\kappa} (\mathcal{G}\mathcal{G}^\dagger)^{-1}, \quad (4.29)$$

where κ denotes the condition number of $\mathcal{G}\mathcal{G}^\dagger$ (assumed to be known). Next, by employing Lemma 3.1, we can construct block encodings for the matrix products:

$$\frac{\mathcal{G}\mathcal{R}^\dagger}{\|\mathcal{R}\|_F \|\mathcal{G}\|_F}, \quad \frac{\mathcal{R}\mathcal{G}^\dagger}{\|\mathcal{R}\|_F \|\mathcal{G}\|_F}. \quad (4.30)$$

Finally, leveraging [Lemma 3.3](#), we can construct a block encoding of the complete operator:

$$\frac{\mathcal{B}\mathcal{B}^\dagger + \mathcal{R}\mathcal{R}^\dagger - \mathcal{R}\mathcal{G}^\dagger(\mathcal{G}\mathcal{G}^\dagger)^{-1}\mathcal{G}\mathcal{R}^\dagger}{4\|\mathcal{B}\|_F^2\|\mathcal{R}\|_F^2\|\mathcal{G}\|_F^2\kappa} = \frac{\partial_{r+1}^{K_1, K_2}(\partial_{r+1}^{K_1, K_2})^\dagger}{4\|\mathcal{B}\|_F^2\|\mathcal{R}\|_F^2\|\mathcal{G}\|_F^2\kappa}. \quad (4.31)$$

We have already derived the operator

$$\frac{(\partial_r^{K_1})^\dagger \partial_r^{K_1}}{(r+1)|S_r^{K_1}|} \quad (4.32)$$

in the previous section. Therefore, we may once again invoke [Lemma 3.3](#) to construct a block encoding of the operator

$$\frac{\partial_{r+1}^{K_1, K_2}(\partial_{r+1}^{K_1, K_2})^\dagger + (\partial_r^{K_1})^\dagger \partial_r^{K_1}}{8(r+1)|S_r^{K_1}| \cdot \|\mathcal{B}\|_F^2\|\mathcal{R}\|_F^2\|\mathcal{G}\|_F^2\kappa}. \quad (4.33)$$

Next, we analyze the Frobenius norms of the matrices \mathcal{B} , \mathcal{R} , and \mathcal{G} . The blue block \mathcal{B} corresponds to $\partial_{r+1}^{K_1}$ and has dimensions $|S_r^{K_1}| \times |S_{r+1}^{K_1}|$. Each column contains $(r+1)$ nonzero entries, all equal to 1, and hence, $\|\mathcal{B}\|_F^2 = (r+1)|S_{r+1}^{K_1}|$. The red block \mathcal{R} has dimensions $|S_r^{K_1}| \times (|S_{r+1}^{K_2}| - |S_{r+1}^{K_1}|)$, with at most $(r+1)$ nonzero entries per row, each equal to 1. Therefore, its Frobenius norm satisfies

$$\|\mathcal{R}\|_F^2 = (r+1)(|S_{r+1}^{K_2}| - |S_{r+1}^{K_1}|). \quad (4.34)$$

Similarly, the green block \mathcal{G} is of size $(|S_r^{K_2}| - |S_r^{K_1}|) \times (|S_{r+1}^{K_2}| - |S_{r+1}^{K_1}|)$, and each column contains at most $(r+1)$ entries equal to 1, yielding

$$\|\mathcal{G}\|_F^2 = (r+1)(|S_{r+1}^{K_2}| - |S_{r+1}^{K_1}|). \quad (4.35)$$

Combining these, we find that the denominator of the normalized operator has asymptotic magnitude $\mathcal{O}(r^2|S_r^{K_1}|(|S_{r+1}^{K_2}| - |S_{r+1}^{K_1}|))$. As in the final step of the previous section, we employ the stochastic rank estimation method introduced in [[US16](#), [USS17](#), [UAS⁺21](#)] to approximate the normalized r -th persistent Betti number,

$$\frac{\beta_r^{\text{persistent}}}{|S_r^{K_1}|} = 1 - \frac{\text{rank}(\partial_{r+1}^{K_1, K_2}(\partial_{r+1}^{K_1, K_2})^\dagger + (\partial_r^{K_1})^\dagger \partial_r^{K_1})}{|S_r^{K_1}|}, \quad (4.36)$$

to additive accuracy ϵ . The overall computational complexity required to achieve this accuracy is

$$\mathcal{O}\left(\frac{\log\left(r^2|S_r^{K_1}|(|S_{r+1}^{K_2}| - |S_{r+1}^{K_1}|)\right)\left(\log^2(1/\epsilon)\log\left(r(|S_{r+1}^{K_2}| - |S_{r+1}^{K_1}|)\right) + \log\left(r|S_r^{K_1}|\right)\right)}{\epsilon^2}\right). \quad (4.37)$$

5 Homology property testing

5.1 Triviality testing

While our proposed algorithm and previous efforts [[SL23](#), [Hay22](#), [BSG⁺24](#), [MGB22](#)] primarily concentrate on the estimation of (normalized) Betti numbers, we now turn our attention to a closely related and fundamentally significant problem in algebraic topology. Specifically, we consider the problem of verifying whether a given r -cycle belongs to the trivial homology class.

Recall that the r -th homology group of a simplicial complex K is defined as the quotient $H_r^K = Z_r^K / B_r^K$, where Z_r^K is the group of r -cycles and B_r^K is the group of r -boundaries. This quotient endows Z_r^K with

an equivalence relation: two r -cycles are homologous if their difference lies in B_r^K . Each equivalence class under this relation is referred to as a homology class. The dimension of H_r^K , namely the r -th Betti number β_r , counts the number of linearly independent homology classes. Consequently, identifying all such classes is a #P-hard problem.

Instead of attempting to enumerate all homology classes, we focus on a restricted variant of this problem: determining whether a given r -cycle c_r is homologous to zero, i.e., whether c_r represents the trivial homology class. The trivial homology class consists of all cycles that are themselves boundaries of some $(r+1)$ -chain. In formal terms, c_r is null-homologous if there exists a chain c_{r+1} such that

$$c_r = \partial_{r+1} c_{r+1}, \quad (5.1)$$

where ∂_{r+1} denotes the $(r+1)$ -st boundary operator.

Let $S_r^K = \{\sigma_{r_i}\}_{i=1}^{|S_r^K|}$ be the set of r -simplices in the complex K . We represent each simplex σ_{r_i} by the computational basis state $|i\rangle$ in a Hilbert space of $\log |S_r^K|$ qubits. Let $C = \{i_1, i_2, \dots, i_L\} \subseteq \{1, \dots, |S_r^K|\}$ be the index set of simplices comprising c_r , with $0 \leq L \leq |S_r^K|$. The r -cycle is then encoded as

$$c_r = \sum_{i_j \in C} |i_j\rangle. \quad (5.2)$$

Given that the constituent simplices of c_r are known, the vector representation of c_r is sparse, with ones at the positions corresponding to the indices in C .

To determine whether c_r is null-homologous, it suffices to check whether the linear system Eq. (5.1) admits a solution. This is equivalent to verifying whether c_r lies in the column space (image) of ∂_{r+1} . In linear algebraic terms, this holds if and only if the augmented matrix $[\partial_{r+1}|c_r]$ has the same rank as ∂_{r+1} . We leverage the Lemma 3.6 to estimate the rank of both ∂_{r+1} and the augmented matrix $[\partial_{r+1}|c_r]$. If the estimated ranks match up to the allowed accuracy ϵ , we conclude that c_r lies in the image of ∂_{r+1} with high confidence. Hence, the quantum algorithm enables us to test null-homology for a given r -cycle efficiently, even when the problem is embedded in high-dimensional simplicial complexes.

In the previous section, we obtained the block encoding of

$$\frac{\partial_{r+1}^\dagger \partial_{r+1}}{(r+2)|S_{r+1}^K|}. \quad (5.3)$$

A direct application of the Lemma 3.6 enables estimation of the ratio

$$\frac{\text{rank}(\partial_{r+1}^\dagger \partial_{r+1})}{|S_{r+1}^K|} = \frac{\text{rank}(\partial_{r+1})}{|S_{r+1}^K|} \quad (5.4)$$

to additive precision ϵ , since $\text{rank}(\partial_{r+1}) = \text{rank}(\partial_{r+1}^\dagger \partial_{r+1})$.

Let λ_1 denote the smallest nonzero eigenvalue of Eq. (5.3). Owing to the normalization factor $(r+2)|S_{r+1}^K|$, it is reasonable to expect $\lambda_1^{-1} = \mathcal{O}((r+2)|S_{r+1}^K|)$. Since the block encoding of Eq. (5.3) can be implemented with complexity $\mathcal{O}(\log(r|S_{r+1}^K|))$ by Lemma 4.1, the overall time complexity for estimating the ratio $\text{rank}(\partial_{r+1})/|S_{r+1}^K|$ to precision ϵ is

$$\mathcal{O}\left(\frac{\log(r|S_{r+1}^K|) \log((r+2)|S_{r+1}^K|)}{\epsilon^2}\right). \quad (5.5)$$

Next, consider the matrix $\partial_* := [\partial_{r+1}|c_r]$, formed by appending the column vector c_r to ∂_{r+1} . The resulting matrix has dimension $|S_r^K| \times (|S_{r+1}^K| + 1)$. Once the cycle c_r of interest is specified, that is, the set

of r -simplices $C = \{i_1, i_2, \dots, i_L\}$ comprising c_r is given, its vector representation is known. The ℓ_2 -norm of c_r is then \sqrt{L} , and the Frobenius norm of ∂_* becomes $\|\partial_*\|_F = ((r+2)|S_{r+1}^K| + L)^{1/2}$.

Applying [Lemma 4.1](#) yields a block encoding of the normalized operator

$$\frac{\partial_*^\dagger \partial_*}{(r+2)|S_{r+1}^K| + L} \quad (5.6)$$

with complexity $\mathcal{O}((r+1)(|S_{r+1}^K| + 1)) = \mathcal{O}(r|S_{r+1}^K|)$. Let λ_2 denote the smallest nonzero eigenvalue of [Eq. \(5.6\)](#). Then, $\lambda_2^{-1} = \mathcal{O}((r+2)|S_{r+1}^K| + L)$. By [Lemma 3.6](#), the rank ratio

$$\frac{\text{rank}(\partial_*^\dagger \partial_*)}{|S_{r+1}^K| + 1} = \frac{\text{rank}(\partial_*)}{|S_{r+1}^K| + 1} \quad (5.7)$$

can be estimated to additive precision ϵ with time complexity

$$\mathcal{O}\left(\frac{\log(r|S_{r+1}^K|) \log((r+2)|S_{r+1}^K| + L)}{\epsilon^2}\right). \quad (5.8)$$

We remark that comparing the ratios $\text{rank}(\partial_{r+1})/|S_{r+1}^K|$ and $\text{rank}(\partial_*)/(|S_{r+1}^K| + 1)$ is insufficient to infer a potential change in the rank of the matrix upon appending the column vector c_r . To rigorously determine whether the rank has increased (e.g., by 1), it is necessary to estimate both $\text{rank}(\partial_{r+1})$ and $\text{rank}(\partial_*)$ to a multiplicative accuracy δ . This necessitates setting the estimation precision parameter ϵ from the previous procedures to

$$\delta \cdot \frac{\text{rank}(\partial_{r+1})}{|S_{r+1}^K|} \quad \text{and} \quad \delta \cdot \frac{\text{rank}(\partial_*)}{|S_{r+1}^K| + 1},$$

respectively.

With access to such multiplicative approximations, one can reliably determine whether the addition of c_r changes the rank of the boundary matrix ∂_{r+1} . The total complexity of this procedure is the sum of the complexities of estimating the rank of ∂_{r+1} and of ∂_* . Hence, the overall time complexity is

$$\mathcal{O}\left(\frac{\log(r|S_{r+1}^K|) \log((r+2)|S_{r+1}^K| + L) |S_{r+1}^K|^2}{\delta^2 (\text{rank}(\partial_{r+1}))^2}\right). \quad (5.9)$$

Here, note that setting δ to be a constant still ensures that the testing algorithm succeeds with high probability.

Classically, one may directly compute the ranks of ∂_{r+1} and ∂_* using Gaussian elimination, which has a time complexity of $\mathcal{O}(|S_{r+1}^K|^3)$. Thus, for the quantum algorithm to offer a genuine computational advantage, the rank of ∂_{r+1} must be on the order of $|S_{r+1}^K|$. This is in contrast with the setting considered in previous works (e.g., [\[LGZ16, SL23, BSG⁺24\]](#)), where the quantum advantage in estimating Betti numbers becomes manifest when the Betti number is large, i.e., when $\beta_r \sim |S_r^K|$.

We now investigate the condition under which $\text{rank}(\partial_{r+1}) \approx |S_{r+1}^K|$. Recall that the $(r+1)$ -st combinatorial Laplacian is defined as $\Delta_{r+1} = \partial_{r+2} \partial_{r+2}^\dagger + \partial_{r+1}^\dagger \partial_{r+1}$, and that its kernel has dimension equal to the $(r+1)$ -st Betti number, β_{r+1} . Since Δ_{r+1} is the sum of two positive semidefinite operators, its kernel is contained in the intersection of the kernels of these two terms, implying $\beta_{r+1} \leq \dim \ker(\partial_{r+1}^\dagger \partial_{r+1})$. Moreover, as $\partial_{r+1}^\dagger \partial_{r+1}$ is Hermitian and positive semidefinite, we have the decomposition

$$\dim \ker(\partial_{r+1}^\dagger \partial_{r+1}) + \text{rank}(\partial_{r+1}^\dagger \partial_{r+1}) = |S_{r+1}^K|. \quad (5.10)$$

Since $\text{rank}(\partial_{r+1}^\dagger \partial_{r+1}) = \text{rank}(\partial_{r+1})$, it follows that if $\text{rank}(\partial_{r+1}) \approx |S_{r+1}^K|$, then

$$\dim \ker(\partial_{r+1}^\dagger \partial_{r+1}) \ll |S_{r+1}^K| \Rightarrow \beta_{r+1} \ll |S_{r+1}^K|. \quad (5.11)$$

Consequently, the proposed quantum algorithm for testing the triviality of a homology class performs optimally in the regime where the Betti numbers are small—e.g., in configurations such as low-genus surfaces. This is in direct contrast to the quantum algorithms for Betti number estimation discussed in [Section 4.2](#), which exhibit optimal performance in the high Betti number regime.

5.2 Equivalence testing

As previously discussed, the zero homology class represents the simplest case, consisting solely of trivial r -cycles. The procedure outlined above enables us to determine whether a given cycle is homologous to zero. Specifically, if the linear system $\partial_{r+1} c_{r+1} = c_r$ has no solution, then c_r is not a boundary, and hence not homologous to zero. In this case, c_r must represent a non-trivial homology class.

The solution relies on the fact that two r -cycles are homologous if and only if their difference is a boundary. That is, $c_1 \sim c_2$ if and only if there exists a $(r+1)$ -chain $c_{r+1} \in C_{r+1}^K$ such that $\partial_{r+1} c_{r+1} = c_1 - c_2$. Suppose that classical descriptions of c_1 and c_2 are given. As in the previous case, let C_1 and C_2 denote the sets of r -simplices supporting c_1 and c_2 , respectively. Then the entries of the vectors c_1 and c_2 are classically accessible, and hence so are the entries of $c_1 - c_2$.

To determine whether $c_1 - c_2$ is a boundary, we check whether the linear system $\partial_{r+1} c_{r+1} = c_1 - c_2$ has a solution. As in the zero-class case, this can be done by comparing the ranks of ∂_{r+1} and the augmented matrix $[\partial_{r+1} | (c_1 - c_2)]$. Therefore, the computational complexity of this procedure is identical to that of verifying zero-homology, as previously discussed.

5.3 Tracking homology classes

The preceding sections were devoted to the problem of testing whether a given cycle is homologous to zero, or whether two given cycles are homologous to each other. Meanwhile, as discussed in [Section 3.3](#), the central problem in topological data analysis (TDA) is the estimation of (persistent) Betti numbers associated with a simplicial complex. This task has been shown to be NP-hard [[SL23](#)], thereby ruling out the possibility of an exponential quantum speed-up for generic inputs. As a result, significant asymptotic improvements through quantum algorithms for Betti number estimation appear unlikely.

Motivated by the techniques developed in our preceding analysis, we now consider whether they can provide utility within the broader framework of TDA. In [Section 4.3](#), we introduced the concept of persistent Betti numbers and their topological significance. In particular, the r -th persistent homology group encodes information about r -dimensional features that persist between two filtration scales. The rank of this group, the persistent Betti number, quantifies the number of such features. Intuitively, features that appear only within a narrow range of filtration values are considered topological noise, whereas those that persist across a wide range are interpreted as robust, intrinsic structures of the underlying dataset.

Inspired by this perspective, we propose a cycle-centric approach: rather than estimating persistent Betti numbers directly, we track the homological behavior of a specific cycle across filtration scales. To this end, suppose we are given three simplicial complexes $K_1 \subseteq K_2 \subseteq K_3$ obtained at increasing filtration values. Let c_r be an r -cycle in K_1 —and hence also in K_2 and K_3 , since the inclusion of simplices preserves cycles.

Note that the boundary maps at each filtration scale differ, and we denote them as $\partial_{r+1}^{K_1}$, $\partial_{r+1}^{K_2}$, and $\partial_{r+1}^{K_3}$, respectively. By applying the zero-homology testing algorithm from [Section 5.1](#) to each of these maps,

we can determine whether c_r is homologous to zero at each scale. For instance, if c_r is not a boundary in K_1 but becomes a boundary in K_2 and K_3 , then we observe that the homology class containing c_r appears at the first scale and disappears in the later ones—precisely the type of topological change captured by persistent homology.

Similarly, we may apply the algorithm from [Section 5.2](#) to compare the homological relationship between two cycles c_1 and c_2 at various filtration levels. Suppose that $c_1 \sim c_2$ in K_1 , but not in K_2 . Then at least one of the cycles must transition into a different homology class, indicating a change in the topological structure of the complex. This method therefore provides a complementary approach to analyzing persistent topological features—not by computing Betti numbers directly, but by tracking individual cycles through the filtration. Such cycle-based methods may offer additional insights or computational advantages in scenarios where specific cycles are of interest or where the homology classes themselves carry semantic meaning.

5.4 From testing homology class to estimating Betti numbers

In the preceding sections, we have shown that quantum algorithms can determine whether two given cycles belong to the same homology class. Furthermore, we have argued that such algorithms can be leveraged to track homology classes across varying length scales, i.e., over a filtration of a simplicial complex of interest. The appearance or disappearance of a homology class may indicate a change in the underlying topological structure; hence, the ability to track individual homology classes can be interpreted as the capability to detect topological changes in the dataset. For instance, a homology class that appears at a particular length scale but disappears shortly thereafter may reasonably be regarded as topological noise.

Motivated by this observation, we extend our consideration to a more general problem: *tracking Betti numbers*. At first glance, this seems closely related to the context of [Section 4.3](#), in which we considered the estimation of persistent Betti numbers. These quantities, by definition, count the number of homology classes that persist across a range of filtration values. However, persistent Betti numbers capture the topological features of the entire complex in a *global* manner, which can be computationally demanding. In contrast, our approach focuses on *local* structure, thereby narrowing the scope and potentially reducing the computational overhead. The underlying expectation is that local analysis of homological features can effectively reveal global topological changes with less effort.

Suppose that at a given filtration level, corresponding to a simplicial complex K_1 , we are given a collection of r -cycles $c_{r_1}, c_{r_2}, \dots, c_{r_s}$. Using the algorithm presented in [Section 5.2](#), we can determine whether any pair among them belongs to the same homology class. By performing such comparisons, we group homologous cycles together and select one representative from each group. Without loss of generality, let these representatives (modulo boundaries) be denoted $c_{r_1}^h, c_{r_2}^h, \dots, c_{r_p}^h$, where $p \leq s$. These representatives are elements of the homology group H_r , and the r -th Betti number β_r is defined as the dimension of H_r . By definition, the dimension of a vector space corresponds to the maximal number of linearly independent elements in it. Therefore, if we can determine the number of linearly independent vectors among the set $\{c_{r_1}^h, c_{r_2}^h, \dots, c_{r_p}^h\}$, we can infer the dimension of a subspace of H_r .

To that end, we organize these vectors into a matrix

$$\mathcal{C} = [c_{r_1}^h, c_{r_2}^h, \dots, c_{r_p}^h], \quad (5.12)$$

where the rank of \mathcal{C} is precisely the number of linearly independent cycles among the given representatives. Since these vectors are assumed to be classically known, we can apply [Lemma 4.1](#) to construct a block-encoding of the normalized Gram matrix $\mathcal{C}^\dagger \mathcal{C} / \|\mathcal{C}\|_F^2$, where the normalization by the Frobenius norm ensures that the spectral norm is bounded. This matrix is of dimension $p \times p$ and shares the same rank as \mathcal{C} . Hence, our goal reduces to estimating the rank of this matrix.

As discussed in [Section 4.2](#), several techniques exist for estimating the rank of a Hermitian matrix. Among them, the stochastic rank estimation algorithm [[US16](#), [USS17](#), [UAS⁺21](#)] is particularly well-suited for our setting. It allows us to estimate the ratio

$$\frac{1}{p} \cdot \text{rank} \left(\frac{C^\dagger C}{\|C\|_F^2} \right) \quad (5.13)$$

to within additive error ϵ in time complexity

$$\mathcal{O} \left(\frac{\log(\lambda_{\min}(C^\dagger C / \|C\|_F^2))}{\epsilon^2} \right), \quad (5.14)$$

where $\lambda_{\min}(C^\dagger C / \|C\|_F^2)$ denotes the smallest nonzero eigenvalue of the matrix $C^\dagger C / \|C\|_F^2$. Consequently, we can directly infer the desired ratio $\text{rank}(C)/p$, which provides an estimate of the number of linearly independent homology representatives.

We emphasize that the vectors $c_{r_1}^h, c_{r_2}^h, \dots, c_{r_p}^h$ belong to the (sub)space H_r , whose dimension is precisely the r th Betti number β_r . Thus, the number of linearly independent such vectors yields a lower bound on β_r , and in favorable cases, may even yield its exact value. This strategy therefore offers an alternative route to computing Betti numbers, supplementing the conventional approach based on combinatorial Laplacians, as reviewed in [Section 3.2](#).

5.5 Cycle detection

As in [Section 5.1](#), let the indices of the r -simplices involved in c_r be denoted by the index set $C := \{i_1, i_2, \dots, i_L\}$, so that the r -chain can be formally written as

$$c_r = \sum_{i \in C} |i\rangle. \quad (5.15)$$

By definition, c_r is an r -cycle if and only if $\partial_r c_r = 0$. Hence, to verify whether c_r is a cycle, it suffices to examine the action of the boundary operator ∂_r on c_r .

As discussed in [Lemma 4.1](#), given a classical description of the simplicial complex $\{S_r\}$, one can block-encode the operator

$$\frac{\partial_r^\dagger \partial_r}{(r+1)|S_r^K|} \quad (5.16)$$

into a unitary operator, which we denote as U_r .

Moreover, since the elements of the index set C are classically known, we can apply the method of [[ZLY22](#)] to prepare the quantum state

$$|c_r\rangle = \frac{1}{\sqrt{L}} \sum_{i \in C} |i\rangle, \quad (5.17)$$

using a quantum circuit of depth $\mathcal{O}(\log(L))$.

We now apply the unitary U_r to the state $|0\rangle |c_r\rangle$, where $|0\rangle$ denotes the ancilla qubits required for the block-encoding construction. According to [Definition 3.1](#) and [Eq. \(3.4\)](#), we have

$$U_r |0\rangle |c_r\rangle = |0\rangle \cdot \frac{\partial_r^\dagger \partial_r}{(r+1)|S_r^K|} |c_r\rangle + |\text{Garbage}\rangle, \quad (5.18)$$

where $|\text{Garbage}\rangle$ is orthogonal to the $|0\rangle$ -component and takes the form

$$|\text{Garbage}\rangle = \sum_{i \neq 0} |i\rangle |\text{Redundant}_i\rangle, \quad (5.19)$$

with $|\text{Redundant}_i\rangle$ denoting unnormalized and irrelevant residual states. Now, if c_r is indeed a cycle, then $\partial_r |c_r\rangle = 0$, and thus $\partial_r^\dagger \partial_r |c_r\rangle = 0$. This implies that the entire amplitude of the $|0\rangle$ component vanishes, and the resulting state is orthogonal to $|0\rangle$ in the ancilla register. Therefore, if we measure the ancilla qubits and never observe the outcome $|0\rangle$, we can infer that c_r is a cycle.

To make this inference statistically meaningful, we repeat the process T times. If the outcome $|0\rangle$ is never observed, then we can conclude, with success probability $1 - \eta$, that c_r is a cycle. It suffices to take $T = \mathcal{O}(1/\eta)$. Thus, we obtain a *probabilistic quantum algorithm* for verifying whether a given chain is a cycle.

6 Cohomology and applications

6.1 An overview of cohomology

As discussed in [Section 3.2](#) and [Section 3.3](#), we introduced several foundational concepts in algebraic topology, including the r -simplex σ_r (for $r \in \mathbb{Z}_+$), r -chains c_r (formal linear combinations of r -simplices), and the r -th chain group C_r^K of a simplicial complex K . For brevity, we drop the superscript K and denote the r -chain group simply by C_r . These objects form the backbone of homology theory.

Cohomology theory, in contrast, centers on *cochains*, which are linear functionals mapping chains to real numbers. Formally, an r -th cochain ω^r is a map $\omega^r : C_r \rightarrow \mathbb{R}$. The set of all r -th cochains, denoted C^r , forms a vector space over \mathbb{R} with the natural additive structure:

$$(\omega_1^r + \omega_2^r)(c_r) = \omega_1^r(c_r) + \omega_2^r(c_r), \quad \forall c_r \in C_r. \quad (6.1)$$

In analogy with the boundary operator in homology, $\partial_r : C_r \rightarrow C_{r-1}$, cohomology introduces the *coboundary* operator, $\delta^r : C^r \rightarrow C^{r+1}$. This operator is defined via duality: for any $c_{r+1} \in C_{r+1}$ and $\omega^r \in C^r$, $\delta^r \omega^r(c_{r+1}) := \omega^r(\partial_{r+1}(c_{r+1}))$. This definition is well-posed since $\partial_{r+1}(c_{r+1}) \in C_r$, and ω^r acts on elements of C_r . A fundamental fact is that the matrix representation of δ^r is the transpose (or adjoint) of ∂_{r+1} . $\delta^r = \partial_{r+1}^\dagger$.

We now mirror the homological concepts in the cohomological setting. An r -chain c_r is called a *cycle* if $\partial_r c_r = 0$. Analogously, an r -cochain ω^r is called a *cocycle* if $\delta^r \omega^r = 0$. The set of all r -cocycles forms the cocycle group Z^r . A cochain ω^r is called a *coboundary* if there exists $\omega^{r-1} \in C^{r-1}$ such that $\omega^r = \delta^{r-1} \omega^{r-1}$. The set of all r -coboundaries forms the coboundary group B^r . It is a standard result that the coboundary operators satisfy $\delta^r \delta^{r-1} = 0$, implying $B^r \subseteq Z^r$. The r -th cohomology group is then defined as the quotient: $H^r := Z^r / B^r$. A central theorem in algebraic topology asserts that the cohomology and homology groups are isomorphic: $H^r \cong H_r$, which illustrates the duality between cohomology and homology. In particular, this isomorphism implies that Betti numbers can equivalently be computed via the spectrum of coboundary operators.

Let us now consider the space C^r of r -cochains, which has dimension $|S_r|$, the number of r -simplices in K . Let $\{e_i\}_{i=1}^{|S_r|}$ denote a basis of C^r such that for the j -th r -simplex $\sigma_{r,j}$, the basis element e_i satisfies $e_i(\sigma_{r,j}) = \delta_{ij}$. Any cochain $\omega^r \in C^r$ can then be expressed as:

$$\omega^r = \sum_{i=1}^{|S_r|} \omega_i^r e_i, \quad (6.2)$$

where $\omega_i^r \in \mathbb{R}$. For a general r -chain $c_r \in C_r$ written as

$$c_r = \sum_{j=1}^{|S_r|} (c_r)_j \sigma_{r_j}, \quad (6.3)$$

the evaluation of ω^r on c_r is:

$$\omega^r(c_r) = \sum_{i=1}^{|S_r|} \omega_i^r e_i(c_r) = \sum_{i=1}^{|S_r|} \omega_i^r e_i \left(\sum_{j=1}^{|S_r|} (c_r)_j \sigma_{r_j} \right) = \sum_{i=1}^{|S_r|} \sum_{j=1}^{|S_r|} \omega_i^r (c_r)_j \delta_{ij} = \sum_{i=1}^{|S_r|} \omega_i^r (c_r)_i. \quad (6.4)$$

This inner product representation provides a concrete numerical interpretation of cochain action on chains under the canonical basis.

6.2 Cohomological frameworks for constructing r -cocycles

In the previous section, we introduced the foundational notions of cohomology theory. In particular, we defined an r -cochain ω^r as a linear functional that maps an arbitrary r -chain to a real number. An r -cochain ω^r is called an r -cocycle if it lies in the kernel of the coboundary operator δ^r , i.e., $\delta^r \omega^r = 0$. Meanwhile, an r -cochain is an r -coboundary if it lies in the image of the coboundary operator on $(r-1)$ -cochains, i.e., $\omega^r = \delta^{r-1} \omega^{r-1}$ for some $(r-1)$ -cochain ω^{r-1} .

The r -th cohomology group is then defined as the quotient

$$H^r := \frac{\ker(\delta^r)}{\text{im}(\delta^{r-1})}, \quad (6.5)$$

which imposes an equivalence relation: two r -cocycles are cohomologous if their difference is an r -coboundary. That is, $\omega_1^r \sim \omega_2^r$ if and only if $\omega_1^r - \omega_2^r = \delta^{r-1} \omega^{r-1}$ for some ω^{r-1} . The cohomology group H^r thus consists of equivalence classes of r -cocycles modulo coboundaries, analogous to how r -cycles modulo boundaries form homology groups, as discussed in [Section 3.2](#), [Section 5.1](#), and [Section 5.2](#).

An important property of cohomology is that any r -cocycle ω^r maps homologous r -cycles to the same real value. To see this, let c_{r_1}, c_{r_2} be two r -cycles such that they are homologous, i.e., there exists an $(r+1)$ -chain c_{r+1} with $c_{r_1} - c_{r_2} = \partial_{r+1} c_{r+1}$. Then for any r -cocycle ω^r , we compute:

$$\omega^r(c_{r_1}) = \omega^r(c_{r_2} + \partial_{r+1} c_{r+1}) \quad (6.6)$$

$$= \omega^r(c_{r_2}) + \omega^r(\partial_{r+1} c_{r+1}) \quad (6.7)$$

$$= \omega^r(c_{r_2}) + (\delta^r \omega^r)(c_{r+1}). \quad (6.8)$$

Since ω^r is a cocycle, $\delta^r \omega^r = 0$, hence $\omega^r(c_{r_1}) = \omega^r(c_{r_2})$. In other words, the value of ω^r on a cycle depends only on its homology class. This observation motivates us to ask whether a similar invariance holds for cohomologous cocycles.

Let ω_1^r and ω_2^r be two cohomologous r -cocycles, i.e., there exists an $(r-1)$ -cochain ω^{r-1} such that

$$\omega_1^r - \omega_2^r = \delta^{r-1} \omega^{r-1}. \quad (6.9)$$

We evaluate both cocycles on an arbitrary r -cycle c_r :

$$\omega_1^r(c_r) = \omega_2^r(c_r) + (\delta^{r-1} \omega^{r-1})(c_r) \quad (6.10)$$

$$= \omega_2^r(c_r) + \omega^{r-1}(\partial_r c_r) \quad (6.11)$$

$$= \omega_2^r(c_r), \quad (6.12)$$

since c_r is a cycle and thus $\partial_r c_r = 0$. Therefore, cohomologous cocycles agree on all cycles. Consequently, we may regard cohomology classes as functionals on homology classes. This leads to the key insight:

Remark 6.1. *A cohomology class defines a well-defined linear functional on homology classes.*

Such properties reveal the deep duality between homology and cohomology. Equivalence relations are imposed respectively on cycles and cocycles via boundaries and coboundaries, and the topological structure of the underlying complex is revealed through how these classes interact. The duality described above motivates a reformulation of the homology testing problem using cohomological language.

Thanks to the established duality, we know that for any r -cocycle ω^r , the difference $\omega^r(c_{r_1}) - \omega^r(c_{r_2})$ depends only on the homology class of $c_{r_1} - c_{r_2}$. In particular, $c_{r_1} \sim c_{r_2}$ if and only if $\omega^r(c_{r_1}) = \omega^r(c_{r_2})$ for all cocycles ω^r , or equivalently, for all cohomology classes $[\omega^r] \in H^r$. Therefore, we obtain the following criterion:

Remark 6.2. *Two r -cycles are homologous if and only if all r -cocycles evaluate them equally.*

This cohomological lens offers not only a theoretical foundation but also a potential algorithmic strategy, particularly in settings where cocycles can be efficiently computed or represented, such as in persistent cohomology or combinatorial Hodge theory.

As outlined in [Section 5.2](#), the homological approach to testing whether two r -cycles c_{r_1} and c_{r_2} are homologous relies on the definition that they differ by a boundary. That is, there exists a $(r+1)$ -chain c_{r+1} such that $c_{r_1} - c_{r_2} = \partial_{r+1}c_{r+1}$. This provides a constructive means of certification: finding such a c_{r+1} is sufficient to conclude that $c_{r_1} \sim c_{r_2}$. In contrast, the cohomological perspective is built upon the dual statement we proved earlier, namely, that for any r -cocycle ω^r , one has $\omega^r(c_{r_1}) = \omega^r(c_{r_2})$ if $c_{r_1} \sim c_{r_2}$. This leads to the natural question:

How does one obtain an r -cocycle, or at least the values $\omega^r(c_{r_1})$ and $\omega^r(c_{r_2})$?

This question is crucial for utilizing the cohomological viewpoint as a computational tool.

Following the same approach as in the previous section, we consider an explicit representation of the r -cocycle ω^r . Let $\{e_i\}_{i=1}^{|S_r|}$ be an orthonormal basis for the cochain group C^r (the dual space of r -chains). Then ω^r can be written as:

$$\omega^r = \sum_{i=1}^{|S_r|} \omega_i^r e_i, \quad (6.13)$$

where each $\omega_i^r \in \mathbb{R}$ represents the coefficient corresponding to basis functional e_i . In vector notation, we express this as:

$$\omega^r = \begin{pmatrix} \omega_1^r \\ \omega_2^r \\ \vdots \\ \omega_{|S_r|}^r \end{pmatrix} \in \mathbb{R}^{|S_r|}. \quad (6.14)$$

To evaluate ω^r on an r -cycle c_r , it suffices to express c_r in the same basis $\{e_i\}$ (via the identification of chains and cochains under the inner product), allowing us to compute $\omega^r(c_r)$ as a dot product $\omega^r(c_r) = \langle \omega^r, c_r \rangle$. Therefore, the action of an r -cocycle on a cycle can be implemented via a linear functional. The key point is that if c_{r_1} and c_{r_2} are not homologous, then there exists some cocycle ω^r such that $\omega^r(c_{r_1}) \neq \omega^r(c_{r_2})$. Consequently, homology detection reduces to finding such a separating cocycle in Z^r (the space of cocycles), or equivalently, testing whether $\omega^r(c_{r_1}) = \omega^r(c_{r_2})$ for all $\omega^r \in Z^r$. We present two methodologies for obtaining the desired r -cocycle using such cohomology functionals.

6.2.1 Constructing block encodings via projection onto $\ker(\delta^r)$

Since the space of r -cocycles is precisely the kernel of the coboundary operator δ^r , i.e., $\ker(\delta^r) \subseteq C^r$, any cochain $\omega^r \in C^r$ can be uniquely decomposed as $\omega^r = \omega_{\text{cycle}}^r + \omega_{\text{non-cycle}}^r$, where $\omega_{\text{cycle}}^r \in \ker(\delta^r)$ and $\omega_{\text{non-cycle}}^r \in \text{im}((\delta^r)^T)$. To project a general cochain ω^r onto the kernel space of δ^r , we define the following projection:

$$\omega_{\text{proj}}^r := \omega^r - (\delta^r)^T (\delta^r (\delta^r)^T)^{-1} \delta^r \cdot \omega^r. \quad (6.15)$$

We verify that this projected vector indeed lies in $\ker(\delta^r)$ by direct computation:

$$\delta^r \omega_{\text{proj}}^r = \delta^r (\omega^r - (\delta^r)^T (\delta^r (\delta^r)^T)^{-1} \delta^r \cdot \omega^r) \quad (6.16)$$

$$= \delta^r \omega^r - \delta^r (\delta^r)^T (\delta^r (\delta^r)^T)^{-1} \delta^r \cdot \omega^r \quad (6.17)$$

$$= \delta^r \omega^r - \delta^r \omega^r = 0. \quad (6.18)$$

Thus, $\omega_{\text{proj}}^r \in \ker(\delta^r)$ as required.

We now consider the matrix representation of δ^r , which, as discussed earlier, is the transpose of the boundary operator ∂_{r+1} . Recall from [Section 4.2](#) that the operator

$$\frac{\partial_{r+1}^\dagger \partial_{r+1}}{(r+2)|S_{r+1}|} \quad (6.19)$$

can be block-encoded efficiently using [Lemma 4.1](#). Since $\delta^r = \partial_{r+1}^T$, we automatically obtain a block encoding of

$$\frac{\delta^r (\delta^r)^T}{(r+2)|S_{r+1}|}. \quad (6.20)$$

A similar construction yields a block encoding of

$$\frac{(\delta^r)^T \delta^r}{(r+2)|S_{r+1}|}. \quad (6.21)$$

Next, we apply [Lemma 4.2](#), which allows for computing the square root of a positive semidefinite block-encoded operator, to obtain a block encoding of

$$\left(\frac{(\delta^r)^T \delta^r}{(r+2)|S_{r+1}|} \right)^{1/2}. \quad (6.22)$$

Finally, we observe the following decomposition of the projection matrix:

$$(\delta^r)^T (\delta^r (\delta^r)^T)^{-1} \delta^r = ((\delta^r)^T \delta^r)^{1/2} \cdot ((\delta^r)^T \delta^r)^{-1} \cdot ((\delta^r)^T \delta^r)^{1/2}. \quad (6.23)$$

This factorization highlights that the projection onto $\text{im}((\delta^r)^T)$ is symmetric and idempotent, and its complement yields a projection onto $\ker(\delta^r)$, which corresponds to the subspace of cocycles.

Now, starting from the block encoding of [Eq. \(6.21\)](#), we apply [Lemma 3.5](#) to obtain a block encoding of its inverse:

$$\frac{1}{\kappa_\delta} ((\delta^r)^T \delta^r)^{-1}, \quad (6.24)$$

where κ_δ denotes the condition number of $(\delta^r)^T \delta^r$. In general, this condition number may be large, making matrix inversion costly. To mitigate this, we invoke the preconditioning technique from [\[CJS13\]](#)

(see [Appendix A](#)), which constructs a matrix A such that AM has bounded condition number, allowing one to invert M efficiently via:

$$M^{-1} = (AM)^{-1}A. \quad (6.25)$$

Assuming A can be constructed as in [\[CJS13\]](#), we first use [Lemma 4.1](#) to block-encode

$$\frac{A^\dagger A}{\|A\|_F^2}. \quad (6.26)$$

Using [Lemma 3.1](#), we obtain a block encoding of

$$\frac{A^\dagger A}{\|A\|_F} \cdot \frac{(\delta^r)^T \delta^r}{(r+2)|S_{r+1}|}. \quad (6.27)$$

Then, applying [Lemma 3.5](#), we get:

$$\frac{1}{\kappa} ((\delta^r)^T \delta^r)^{-1} (A^\dagger A)^{-1}, \quad (6.28)$$

where κ is the condition number of $A^\dagger A \cdot (\delta^r)^T \delta^r$, which is guaranteed to be small by construction. We then multiply with the block encoding of $A^\dagger A / \|A\|_F^2$, resulting in:

$$\frac{((\delta^r)^T \delta^r)^{-1}}{\kappa \|A\|_F^2}. \quad (6.29)$$

Finally, using [Lemma 3.1](#) again with the block encoding of [Eq. \(6.22\)](#), we obtain:

$$\left(\frac{(\delta^r)^T \delta^r}{(r+2)|S_{r+1}|} \right)^{1/2} \cdot \frac{((\delta^r)^T \delta^r)^{-1}}{\kappa \|A\|_F^2} \cdot \left(\frac{(\delta^r)^T \delta^r}{(r+2)|S_{r+1}|} \right)^{1/2} = \frac{(\delta^r)^T (\delta^r (\delta^r)^T)^{-1} \delta^r}{\kappa \|A\|_F^2 (r+2)|S_{r+1}|}. \quad (6.30)$$

This gives us a block encoding of the projection matrix onto $\text{im}((\delta^r)^T)$.

We now turn to computing the projected component of an arbitrary r -cochain ω^r . We randomly generate a unitary U_r of size $|S_r| \times |S_r|$ and use its first column as ω^r . Using [Lemma 3.1](#), we compute a block encoding of:

$$\frac{(\delta^r)^T (\delta^r (\delta^r)^T)^{-1} \delta^r U_r}{\kappa \|A\|_F^2 (r+2)|S_{r+1}|}. \quad (6.31)$$

The first column of this matrix is:

$$\frac{(\delta^r)^T (\delta^r (\delta^r)^T)^{-1} \delta^r \omega^r}{\kappa \|A\|_F^2 (r+2)|S_{r+1}|}. \quad (6.32)$$

Let us define the rescaled cochain

$$(\omega^r)' := \frac{\omega^r}{\kappa \|A\|_F^2 (r+2)|S_{r+1}|}. \quad (6.33)$$

Then the above vector equals

$$(\delta^r)^T (\delta^r (\delta^r)^T)^{-1} \delta^r (\omega^r)'. \quad (6.34)$$

We now use [Lemma 3.4](#) to block-encode

$$\frac{U_r}{\kappa \|A\|_F^2 (r+2)|S_{r+1}|}, \quad (6.35)$$

which contains $(\omega^r)'$ in the first column. Finally, using [Lemma 3.3](#), we compute the block encoding of:

$$\frac{U_r - (\delta^r)^T (\delta^r (\delta^r)^T)^{-1} \delta^r U_r}{2\kappa \|A\|_F^2 (r+2) |S_{r+1}|}, \quad (6.36)$$

whose first column equals

$$\frac{1}{2} ((\omega^r)' - (\delta^r)^T (\delta^r (\delta^r)^T)^{-1} \delta^r (\omega^r)'). \quad (6.37)$$

As shown earlier, this vector lies in $\ker(\delta^r)$, and hence is an r -cocycle. We summarize the above construction as follows:

Lemma 6.1 (Efficient block-encoding of an r -cocycle). *There exists a quantum procedure with time complexity $\mathcal{O}(\log(r|S_r|))$ that returns the unitary block encoding U_c of a matrix whose first column is an r -cocycle $\omega_c^r \in \ker(\delta^r)$.*

6.2.2 Manual construction via explicit representatives

Recall that an r -cocycle ω_c^r belongs to the kernel of δ^r . In other words, for any $(r+1)$ -cochain c_{r+1} , we have

$$\delta^r \omega_c^r(c_{r+1}) = \omega_c^r(\partial_{r+1} c_{r+1}). \quad (6.38)$$

Let $S_{r+1} = \{\sigma_{(r+1)_i}\}_{i=1}^{|S_{r+1}|}$ denote the collection of all $(r+1)$ -simplices. Hence, any $(r+1)$ -cochain can be expressed as

$$c_{r+1} = \sum_{i=1}^{|S_{r+1}|} c_i \sigma_{(r+1)_i}. \quad (6.39)$$

Substituting this expansion into [Eq. \(6.38\)](#), we obtain

$$\delta^r \omega_c^r(c_{r+1}) = \omega_c^r \left(\partial_{r+1} \sum_{i=1}^{|S_{r+1}|} c_i \sigma_{(r+1)_i} \right) = \sum_{i=1}^{|S_{r+1}|} c_i \omega_c^r(\partial_{r+1} \sigma_{(r+1)_i}). \quad (6.40)$$

If ω_c^r is indeed a cocycle, then the left-hand side of the above equation is zero. Consequently, one must have

$$\omega_c^r(\partial_{r+1} \sigma_{(r+1)_i}) = 0, \quad \forall i = 1, 2, \dots, |S_{r+1}|. \quad (6.41)$$

Conversely, if an r -cochain ω_c^r satisfies [Eq. \(6.41\)](#) for every $(r+1)$ -simplex in S_{r+1} , then $\delta^r \omega_c^r(c_{r+1}) = 0$ for all c_{r+1} , so that $\omega_c^r \in \ker(\delta^r)$ and hence is an r -cocycle. The practical challenge is thus:

how can one manually choose an r -cochain ω^r satisfying [Eq. \(6.41\)](#)?

A straightforward strategy is as follows. One iterates over all $(r+1)$ -simplices and assigns real values to the r -simplices lying on their boundaries in such a way that the conditions in [Eq. \(6.41\)](#) hold. Specifically, one may proceed according to the following steps:

- (i) Start with the first $(r+1)$ -simplex $\sigma_{(r+1)_1}$ and consider its boundary $\partial_{r+1} \sigma_{(r+1)_1}$, whose constituent r -simplices are known from the classical description of the boundary operator ∂_{r+1} .
- (ii) Assign arbitrary (e.g., random) real values x_1, x_2, \dots, x_{r+1} to the first r -simplices in the boundary, and then determine the value on the remaining r -simplex by requiring that the sum of the assigned values on the boundary is zero. For example, if the boundary of $\sigma_{(r+1)_1}$ has $(r+2)$ faces, one may set the value for the last face as $1 - (x_1 + x_2 + \dots + x_{r+1})$, so that the boundary condition is met.

- (iii) Next, consider a second $(r+1)$ -simplex $\sigma_{(r+1)_2}$ and similarly assign values on its boundary. When a face is shared with a previously processed simplex, the previously assigned value is re-used.
- (iv) Repeat this procedure until real values have been assigned to all r -simplices in such a way that each $(r+1)$ -simplex satisfies the cocycle condition Eq. (6.41).

This method yields an explicit construction of the desired r -cocycle ω_c^r . Since every $(r+1)$ -simplex is processed and each boundary consists of at most $\mathcal{O}(r)$ faces, the overall classical time complexity for this manual selection process is $\mathcal{O}(r|S_{r+1}|)$. The above selection procedure has complexity $\mathcal{O}(r|S_{r+1}|)$. Thus, in practice, it is only efficient when $|S_{r+1}|$ is not large. It turns out that things can be simpler under certain circumstances, which can further optimize the classical preprocessing time. We recall that we are seeking for r -cochain that satisfies the condition:

$$\omega_c^r(\partial_{r+1}\sigma_{(r+1)_i}) = 0, \quad \forall i = 1, 2, \dots, |S_{r+1}|. \quad (6.42)$$

Suppose there exist two r -simplices that are both faces of a common $(r+1)$ -simplex, and furthermore, are not faces of any other $(r+1)$ -simplices. In this case, the matrix S_{r+1} (and equivalently, the boundary matrix ∂_{r+1}) contains two rows—indexed by p and q with $p, q \leq |S_r|$ —each having a single nonzero entry located in the same column, indexed by $k \leq |S_{r+1}|$. The rows indexed by p and q correspond to the r -simplices σ_{r_p} and σ_{r_q} , respectively, both of which are faces of the $(r+1)$ -simplex $\sigma_{(r+1)_k}$. Define a cochain $\omega_c^r \in C^r$ supported only on σ_{r_p} and σ_{r_q} according to the following rule:

- (i) If $(\partial_{r+1})_{p,k} = (\partial_{r+1})_{q,k}$, then set

$$\begin{aligned} \omega_c^r(\sigma_{r_p}) &= -\omega_c^r(\sigma_{r_q}) = 1, \\ \omega_c^r(\sigma_{r_i}) &= 0 \quad \text{for all } i \notin \{p, q\}. \end{aligned}$$

- (ii) If $(\partial_{r+1})_{p,k} = -(\partial_{r+1})_{q,k}$, then set

$$\begin{aligned} \omega_c^r(\sigma_{r_p}) &= \omega_c^r(\sigma_{r_q}) = 1, \\ \omega_c^r(\sigma_{r_i}) &= 0 \quad \text{for all } i \notin \{p, q\}. \end{aligned}$$

The above construction is elementary and can be implemented in nearly constant time, provided such a pair of r -simplices exists.

Once the values $\omega_c^r(\sigma_{r_i})$ on the r -simplices are determined for all $i = 1, 2, \dots, |S_r|$, we can employ the method described in [ZLY22] to prepare a quantum state corresponding to the normalized r -cocycle:

$$|\omega_c^r\rangle = \frac{1}{\omega} \sum_{i=1}^{|S_r|} \omega_c^r(\sigma_{r_i}) |i-1\rangle, \quad (6.43)$$

where the normalization constant is given by

$$\omega = \left(\sum_{i=1}^{|S_r|} \omega_c^r(\sigma_{r_i})^2 \right)^{1/2}. \quad (6.44)$$

Thus, the classical procedure of manual selection can be efficiently interfaced with the quantum state preparation technique for further quantum processing.

6.3 Homology equivalence testing with cohomological frameworks

We now return to our main objective: determining whether two given r -cycles c_{r_1} and c_{r_2} are homologous (Problem 4; homology equivalence testing).

6.3.1 Constructing block encodings via projection onto $\ker(\delta^r)$

As in Section 5.1 and Section 5.2, we denote the indices of the r -simplices contained in c_{r_1} by $C_1 := \{i_1^1, i_2^1, \dots, i_{L_1}^1\}$, and those contained in c_{r_2} by $C_2 := \{i_1^2, i_2^2, \dots, i_{L_2}^2\}$, where $i_j^1, i_j^2 \in \{1, 2, \dots, |S_r|\}$, and $L_1, L_2 \leq |S_r|$ denote the lengths of the cycles c_{r_1} and c_{r_2} , respectively.

Having obtained a block encoding of the r -cocycle ω_c^r , we now seek to evaluate $\omega^r(c_{r_1})$ and $\omega^r(c_{r_2})$. Since $c_{r_1} = \sum_{i \in C_1} \sigma_{r_i}$ and $c_{r_2} = \sum_{i \in C_2} \sigma_{r_i}$, we have

$$\omega^r(c_{r_1}) = \sum_{i \in C_1} \omega^r(\sigma_{r_i}), \quad \omega^r(c_{r_2}) = \sum_{i \in C_2} \omega^r(\sigma_{r_i}). \quad (6.45)$$

Let U_c be a unitary that block-encodes the vector ω_c^r in its first column. Applying U_c to the initial state $|0\rangle |0\rangle_{|S_r|}$, where $|0\rangle$ is an ancilla register used for block encoding and $|0\rangle_{|S_r|}$ denotes the first computational basis state in the $|S_r|$ -dimensional Hilbert space, we obtain

$$U_c |0\rangle |0\rangle_{|S_r|} = |0\rangle |\omega_c^r\rangle + |\text{Garbage}\rangle. \quad (6.46)$$

Knowing the index set $C_1 = \{i_1^1, i_2^1, \dots, i_{L_1}^1\}$, we can use the method proposed in [ZLY22] to construct the quantum state

$$|\phi_1\rangle = \frac{1}{L_1} \sum_{i \in C_1} |i\rangle. \quad (6.47)$$

By appending the ancilla register, we obtain the state $|0\rangle |\phi_1\rangle$. Then, the inner product

$$\langle 0 | \langle \phi_1 | (|0\rangle |\omega_c^r\rangle + |\text{Garbage}\rangle) = \langle \phi_1 | \omega_c^r = \frac{1}{L_1} \sum_{i \in C_1} \omega^r(\sigma_{r_i}) = \frac{1}{L_1} \omega^r(c_{r_1}) \quad (6.48)$$

can be estimated to additive accuracy ϵ using either the Hadamard test or the SWAP test, with circuit complexity $\mathcal{O}(1/\epsilon)$. A similar procedure can be applied to estimate the ratio $\omega^r(c_{r_2})/L_2$. By comparing the two values $\omega^r(c_{r_1})$ and $\omega^r(c_{r_2})$, one can determine whether the corresponding cycles are homologous.

The complexity for preparing the unitary U_c is $\mathcal{O}(\log(r|S_r|))$. Preparing the states $|\phi_1\rangle$ and $|\phi_2\rangle$ requires complexity $\mathcal{O}(\log(L_1))$ and $\mathcal{O}(\log(L_2))$, respectively. The overlap estimation step has complexity $\mathcal{O}(1/\epsilon)$. Hence, the total complexity is given by

$$\mathcal{O}\left(\frac{(\log(r|S_r|) + \log L_1 + \log L_2)}{\epsilon}\right) = \mathcal{O}\left(\frac{\log(r|S_r| \cdot L_1 L_2)}{\epsilon}\right). \quad (6.49)$$

By choosing $\epsilon = \mathcal{O}(1)$, we obtain constant-additive-error estimates of the target quantities, which suffice for the purpose of comparison. Since the maximal values of L_1 and L_2 are at most $|S_r|$, the overall complexity simplifies to $\mathcal{O}(\log(r|S_r|))$.

6.3.2 Manual construction via explicit representatives

Alternatively, by manual selection, the r -cocycle ω_c^r is classically known. Then we use the method in [ZLY22] to prepare the state

$$|\omega_c^r\rangle = \frac{1}{\omega} \sum_{i=1}^{|S_r|} \omega_c^r(\sigma_{r_i}) |i-1\rangle, \quad (6.50)$$

with normalization factor

$$\omega = \left(\sum_{i=1}^{|S_r|} \omega_c^r(\sigma_{r_i})^2 \right)^{1/2}, \quad (6.51)$$

Then we can apply essentially the same procedure to evaluate the action of ω on the two r -cycles c_{r_1}, c_{r_2} . Specifically, the inner product

$$\langle \phi_1 | \omega_c^r \rangle = \frac{1}{\omega L_1} \sum_{i \in C_1} \omega^r(\sigma_{r_i}) = \frac{1}{\omega L_1} \omega^r(c_{r_1}) \quad (6.52)$$

can again be estimated via the Hadamard or SWAP test. The same applies for the estimate of $\omega^r(c_{r_2})/\omega L_2$, after which we compare the results to decide homology equivalence. The complexity of preparing the state $|\omega_c^r\rangle$ is $\mathcal{O}(|S_r|)$. Preparing the states $|\phi_1\rangle$ and $|\phi_2\rangle$ requires complexities $\mathcal{O}(\log(L_1))$ and $\mathcal{O}(\log(L_2))$, respectively. The final overlap estimation step incurs a complexity of $\mathcal{O}(1/\epsilon)$. Therefore, the total complexity is given by

$$\mathcal{O} \left(\frac{(\log |S_r| + \log L_1 + \log L_2)}{\epsilon} \right) = \mathcal{O} \left(\frac{\log(|S_r| \cdot L_1 L_2)}{\epsilon} \right). \quad (6.53)$$

Assuming $\epsilon = \mathcal{O}(1)$, this simplifies to $\mathcal{O}(\log(|S_r| \cdot L_1 L_2))$. Since $L_1, L_2 \leq |S_r|$, we conclude that the total complexity is $\mathcal{O}(\log(|S_r|))$. The time complexity of the classical processing for manual selection is considered separately.

7 Concluding remarks

In this work, we have investigated several novel directions in quantum topological data analysis. Specifically, we proposed and analyzed a new input model for the estimation of Betti numbers and persistent Betti numbers, allowing quantum algorithms to operate under more structured and informative access assumptions. Notably, we introduced a homology tracking method that bypasses the need to explicitly compute the dimension of the kernel of combinatorial Laplacians, which was central to previous approaches. This yields a new framework for Betti number estimation that exhibits striking improvements, particularly in regimes where previous quantum algorithms were only efficient for simplicial complexes with large Betti numbers. Our analysis demonstrates that, under this refined model, quantum algorithms can achieve substantial—and in some regimes, exponential—speedups over the best-known classical methods as well as over prior quantum approaches.

Beyond the computation of Betti numbers, we introduced and studied the homology property testing problem, which, while closely related to Betti number estimation, captures finer structural features of simplicial complexes. We further extended this framework to the cohomological setting and introduced quantum algorithms for homology class testing via cohomology, thereby providing a dual and often computationally advantageous perspective on homological properties. In particular, we showed that both triviality testing and class distinction problems admit efficient quantum algorithms, yielding exponential advantages under certain assumptions. These results deepen the connection between quantum computing and computational topology and suggest that topological invariants—particularly those defined in homology and cohomology—provide a rich domain for demonstrating quantum advantage.

Several promising directions remain open and merit further investigation. One fundamental structure in cohomology is the *cup product*, which equips the cohomology ring $H^*(K)$ with a graded-commutative algebra structure. Whether quantum algorithms can efficiently compute cup products—or, more broadly,

perform cohomological ring operations—remains an intriguing and largely unexplored question. Progress in this direction could have significant implications, not only for quantum topological data analysis, but also for quantum approaches to manifold invariants and higher-order interactions in data.

Given that our cohomology-based framework offers several advantages over existing homology-based methods, it would be highly interesting to identify additional scenarios in which cohomology can be more effectively leveraged within quantum algorithms. In particular, further exploration of cohomology-inspired primitives could open new algorithmic paradigms that remain inaccessible to purely homological techniques.

Furthermore, recent work such as [SRZ⁺25] suggests potential connections between quantum algorithms and categorified invariants such as Khovanov homology or its persistent counterpart, *Persistent Khovanov Homology*. Investigating how such structures might be integrated into or informed by our cohomological framework presents an exciting direction for future research.

Lastly, while current hardness results show that deciding whether the k -th Betti number exceeds a given threshold is PSPACE-complete [Rud24] for clique complexes and #BQP-complete [CK24] for their counting versions, these results do not fully address the complexity of *approximate* computation. This is a critical gap, as most practical applications in topological data analysis only require Betti numbers to be estimated within a bounded error. To date, the only known indication of a potential quantum advantage in approximate computation arises from the DQC1-hardness of generalized chain complexes [CC24], though this result applies to structures more general than those typically used in applied settings. Clarifying the approximation complexity class for Betti numbers thus remains a central open problem with both theoretical and practical significance.

Acknowledgements

J.L. thanks Marcos Crichigno, Kabgyun Jeong and Daun Jung for helpful discussions. N.A.N. acknowledges support from the Center for Distributed Quantum Processing. Part of this work was completed during N.A.N.’s internship at QuEra Computing Inc.

Data availability

This study did not involve the generation or analysis of any datasets.

Competing interests

The authors declare no competing interests.

A Inverting ill-conditioned matrices

In our cohomological approach, there may be cases where computing the inverse of a matrix with a large condition number is required, such as in the derivation of expressions like Eq. (6.24). In the following, we briefly introduce some known algorithms related to this task.

To overcome the practical limitations of the original HHL algorithm [HHL09], such as the dependence on efficient state preparation, post-selection-based solution extraction, and unfavorable scaling with the condition number κ , a fully unitary and observable-aware formulation of the quantum linear system algorithm (QLSA) is employed [CJS13]. This framework enables coherent processing throughout the algorithm and supports various forms of readout that do not require full wavefunction collapse.

The input state $|b\rangle$ is not assumed to be given directly. Instead, an ancilla-assisted state $|b_T\rangle$ is prepared using controlled operations and amplitude encoding techniques. The resulting state takes the form

$$|b_T\rangle = \cos \phi_b |\tilde{b}\rangle |0\rangle_a + \sin \phi_b |b\rangle |1\rangle_a, \quad (\text{A.1})$$

where ϕ_b encodes the overlap between the constructed state and the target vector $|b\rangle$. This preparation avoids the need for an oracle that directly outputs $|b\rangle$, and instead makes use of data oracles that provide individual components b_j via coherent access.

A modified QLSA is then applied in a fully unitary fashion, producing the superposition

$$|\Psi\rangle = \sqrt{1 - \sin^2 \phi_b \sin^2 \phi_x} |\Phi_0\rangle + \sin \phi_b \sin \phi_x |x\rangle |1\rangle_a |1\rangle_a, \quad (\text{A.2})$$

where $|x\rangle = A^{-1} |b\rangle / \|A^{-1} |b\rangle\|$ is the normalized solution to the linear system, and ϕ_x encodes the success amplitude of the inversion procedure. The desired solution is coherently embedded in the subspace where both ancilla qubits are in the state $|1\rangle$.

Information about $|x\rangle$ is extracted through observable-aware readout techniques, without full-state tomography. First, to estimate the overlap $|\langle R|x\rangle|^2$ with a reference state $|R\rangle$, a swap test is performed using a similarly prepared reference superposition $|R_T\rangle$. The resulting probability amplitudes satisfy

$$|\langle R|x\rangle|^2 = \frac{P_{1110} - P_{1111}}{\sin^2 \phi_b \sin^2 \phi_x \sin^2 \phi_r}, \quad (\text{A.3})$$

where P_{111b} denote measurement probabilities conditioned on specific ancilla outcomes.

Second, expectation values of polynomial observables x^n can be estimated by constructing Hamiltonians of the form $H_{r,w} = x^n |x\rangle \langle x|$, implemented via ancilla-assisted controlled rotations.

Third, to access individual solution components x_j , amplitude estimation is applied to the subspace corresponding to the computational basis state $|j\rangle$. This allows estimation of $|x_j|^2$ with quadratically improved sample complexity compared to classical sampling.

To mitigate the dependence on the condition number κ , a classical preconditioning step is employed. Specifically, a sparse approximate inverse (SPAI) preconditioner M is constructed such that $MA \approx I$, allowing the modified linear system $MA|x\rangle = M|b\rangle$ to be solved instead of the original one. Each column \hat{m}_k of M is determined by solving the minimization problem of $\|\hat{A}\hat{m}_k - \hat{e}_k\|_2$, where \hat{e}_k is the k th standard basis vector, subject to a specified sparsity pattern. This sparsity constraint ensures that the resulting preconditioner M is block-encodable and compatible with efficient Hamiltonian simulation techniques. The transformed system benefits from a much smaller effective condition number, i.e., $\kappa(MA) \ll \kappa(A)$, thereby enhancing the efficiency and stability of the quantum algorithm.

B Stochastic rank estimation

Our quantum algorithm frequently requires estimating the rank of certain matrices as a subroutine. Here, we provide a summarized description of the overall procedure for stochastic rank estimation [US16, USS17, UAS⁺21] used for this purpose.

Given a Hermitian matrix A , its rank can be expressed as the trace of a spectral step function $\text{rank}(A) = \text{Tr}(h(A))$, where

$$h(x) := \begin{cases} 1 & x > \delta \\ 0 & \text{otherwise} \end{cases}, \quad (\text{B.1})$$

under the assumption that the smallest nonzero eigenvalue of A is at least δ . The threshold $\delta > 0$ may be either known a priori or estimated using spectral heuristics tailored to the input complex.

To approximate $\text{Tr}(h(A))$, we expand $h(\cdot)$ into a degree- m Chebyshev polynomial:

$$h(A) \approx \sum_{j=0}^m c_j T_j(A), \quad (\text{B.2})$$

where T_j denotes the j -th Chebyshev polynomial of the first kind, and $\{c_j\}$ are the corresponding coefficients. Thus, we approximate $\text{rank}(A)$ via

$$\text{rank}(A) \approx \text{Tr} \left(\sum_{j=0}^m c_j T_j(A) \right) = \sum_{j=0}^m c_j \text{Tr}(T_j(A)). \quad (\text{B.3})$$

To estimate $\text{Tr}(T_j(A))$ without full diagonalization, we employ the stochastic trace estimation technique. Let $|v_1\rangle, \dots, |v_{n_v}\rangle$ be a collection of random vectors satisfying $\mathbb{E}[|v\rangle\langle v|] = \mathbb{I}$; then

$$\text{Tr}(T_j(A)) \approx \frac{1}{n_v} \sum_{l=1}^{n_v} \langle v_l | T_j(A) | v_l \rangle. \quad (\text{B.4})$$

In practice, preparing i.i.d. random vectors is not feasible on near-term quantum hardware. Instead, we employ quantum states derived from randomly selected columns of the Hadamard matrix, which can be efficiently prepared using shallow-depth circuits. Specifically, starting from $|0\rangle^{\otimes n}$, we apply NOT gates conditioned on a random n -bit string and then Hadamard gates on all qubits. This results in a state corresponding to a uniformly random Hadamard column $|h_{c(l)}\rangle$. (An alternative, though more resource-intensive, strategy is to use approximate t -design circuits, which produce quantum states exhibiting t -wise independence. However, for trace estimation, pairwise independence suffices, and thus Hadamard-based sampling is preferred in our implementation.)

Since Chebyshev polynomials satisfy a recurrence relation classically, the corresponding moments $\langle v_l | T_j(A) | v_l \rangle$ are typically computed via a three-term recurrence. In the quantum setting, we instead express $T_j(x)$ as a sum over matrix powers:

$$T_j(x) = \sum_{i=0}^{\lfloor j/2 \rfloor} \frac{(-1)^i 2^{j-(2i+1)} \binom{2i}{i} \binom{j}{2i} x^{j-2i}}{\binom{j-1}{i}}. \quad (\text{B.5})$$

This allows us to evaluate $\langle v_l | T_j(A) | v_l \rangle$ by computing the moments $\mu_l^{(s)} := \langle v_l | A^s | v_l \rangle$ for $0 \leq s \leq j$.

In our case, $A = \Delta_k$ is the combinatorial k -Laplacian. The required powers of Δ_k can be implemented via a sequence of projections and reflections as described in [Section 4](#), enabling efficient moment computation. Combining all components, we estimate

$$\text{rank}(\Delta_k) \approx \frac{1}{n_v} \sum_{l=1}^{n_v} \left[\sum_{j=0}^m c_j \theta_l^{(j)} \right] \quad (\text{B.6})$$

where $\theta_l^{(j)} := \langle v_l | T_j(\Delta_k) | v_l \rangle$.

References

- [BACS07] Dominic W Berry, Graeme Ahokas, Richard Cleve, and Barry C Sanders. Efficient quantum algorithms for simulating sparse hamiltonians. *Communications in Mathematical Physics*, 270(2):359–371, 2007.
- [BC09] Dominic W Berry and Andrew M Childs. Black-box hamiltonian simulation and unitary implementation. *Quantum Information and Computation*, 12:29–62, 2009.
- [BCC⁺15] Dominic W Berry, Andrew M Childs, Richard Cleve, Robin Kothari, and Rolando D Somma. Simulating hamiltonian dynamics with a truncated taylor series. *Physical Review Letters*, 114(9):090502, 2015.
- [BCK15] Dominic W Berry, Andrew M Childs, and Robin Kothari. Hamiltonian simulation with nearly optimal dependence on all parameters. In *2015 IEEE 56th Annual Symposium on Foundations of Computer Science*, pages 792–809. IEEE, 2015.
- [BCOW17] Dominic W Berry, Andrew M Childs, Aaron Ostrander, and Guoming Wang. Quantum algorithm for linear differential equations with exponentially improved dependence on precision. *Communications in Mathematical Physics*, 356:1057–1081, 2017.
- [Ben80] Paul Benioff. The computer as a physical system: A microscopic quantum mechanical hamiltonian model of computers as represented by turing machines. *Journal of Statistical Physics*, 22:563–591, 1980.
- [Ber14] Dominic W Berry. High-order quantum algorithm for solving linear differential equations. *Journal of Physics A: Mathematical and Theoretical*, 47(10):105301, 2014.
- [BSG⁺24] Dominic W Berry, Yuan Su, Casper Gyurik, Robbie King, Joao Basso, Alexander Del Toro Barba, Abhishek Rajput, Nathan Wiebe, Vedran Dunjko, and Ryan Babbush. Analyzing prospects for quantum advantage in topological data analysis. *PRX Quantum*, 5(1):010319, 2024.
- [Bub15] Peter Bubenik. Statistical topological data analysis using persistence landscapes. *Journal of Machine Learning Research*, 16(1):77–102, 2015.
- [BWP⁺17] Jacob Biamonte, Peter Wittek, Nicola Pancotti, Patrick Rebentrost, Nathan Wiebe, and Seth Lloyd. Quantum machine learning. *Nature*, 549(7671):195–202, 2017.
- [CC24] Chris Cade and P Marcos Crichigno. Complexity of supersymmetric systems and the cohomology problem. *Quantum*, 8:1325, 2024.
- [CJS13] B David Clader, Bryan C Jacobs, and Chad R Sprouse. Preconditioned quantum linear system algorithm. *Physical Review Letters*, 110(25):250504, 2013.
- [CK24] Marcos Crichigno and Tamara Kohler. Clique homology is qma 1-hard. *Nature Communications*, 15(1):9846, 2024.
- [CKS17] Andrew M Childs, Robin Kothari, and Rolando D Somma. Quantum algorithm for systems of linear equations with exponentially improved dependence on precision. *SIAM Journal on Computing*, 46(6):1920–1950, 2017.

- [CVB20] Daan Camps and Roel Van Beeumen. Approximate quantum circuit synthesis using block encodings. *Physical Review A*, 102(5):052411, 2020.
- [Deu85] David Deutsch. Quantum theory, the church–turing principle and the universal quantum computer. *Proceedings of the Royal Society of London. A. Mathematical and Physical Sciences*, 400(1818):97–117, 1985.
- [DJ92] David Deutsch and Richard Jozsa. Rapid solution of problems by quantum computation. *Proceedings of the Royal Society of London. Series A: Mathematical and Physical Sciences*, 439(1907):553–558, 1992.
- [Fey18] Richard P Feynman. Simulating physics with computers. In *Feynman and computation*, pages 133–153. CRC Press, 2018.
- [Gro96] Lov K Grover. A fast quantum mechanical algorithm for database search. In *Proceedings of the twenty-eighth annual ACM Symposium on Theory of Computing*, pages 212–219, 1996.
- [GSK⁺24] Casper Gyurik, Alexander Schmidhuber, Robbie King, Vedran Dunjko, and Ryu Hayakawa. Quantum computing and persistence in topological data analysis. *arXiv preprint arXiv:2410.21258*, 2024.
- [GSLW19] András Gilyén, Yuan Su, Guang Hao Low, and Nathan Wiebe. Quantum singular value transformation and beyond: exponential improvements for quantum matrix arithmetics. In *Proceedings of the 51st Annual ACM SIGACT Symposium on Theory of Computing*, pages 193–204, 2019.
- [Hat05] Allen Hatcher. *Algebraic topology*. Cambridge University Press, 2005.
- [Hay22] Ryu Hayakawa. Quantum algorithm for persistent betti numbers and topological data analysis. *Quantum*, 6:873, 2022.
- [HCH24] Ryu Hayakawa, Kuo-Chin Chen, and Min-Hsiu Hsieh. Quantum walks on simplicial complexes and harmonic homology: Application to topological data analysis with superpolynomial speedups. *arXiv preprint arXiv:2404.15407*, 2024.
- [HCT⁺19] Vojtěch Havlíček, Antonio D Córcoles, Kristan Temme, Aram W Harrow, Abhinav Kandala, Jerry M Chow, and Jay M Gambetta. Supervised learning with quantum-enhanced feature spaces. *Nature*, 567(7747):209–212, 2019.
- [HHL09] Aram W Harrow, Avinatan Hassidim, and Seth Lloyd. Quantum algorithm for linear systems of equations. *Physical Review Letters*, 103(15):150502, 2009.
- [IGMD24] Massimiliano Incudini, Casper Gyurik, Riccardo Molteni, and Vedran Dunjko. Testing the presence of balanced and bipartite components in a sparse graph is qma1-hard. *arXiv preprint arXiv:2412.14932*, 2024.
- [Kit95] A Yu Kitaev. Quantum measurements and the abelian stabilizer problem. *arXiv preprint quant-ph/9511026*, 1995.
- [KK24] Robbie King and Tamara Kohler. Gapped clique homology on weighted graphs is qma 1-hard and contained in qma. In *2024 IEEE 65th Annual Symposium on Foundations of Computer Science (FOCS)*, pages 493–504. IEEE, 2024.

- [LC17] Guang Hao Low and Isaac L Chuang. Optimal hamiltonian simulation by quantum signal processing. *Physical Review Letters*, 118(1):010501, 2017.
- [LC19] Guang Hao Low and Isaac L Chuang. Hamiltonian simulation by qubitization. *Quantum*, 3:163, 2019.
- [LGZ16] Seth Lloyd, Silvano Garnerone, and Paolo Zanardi. Quantum algorithms for topological and geometric analysis of data. *Nature communications*, 7(1):1–7, 2016.
- [Lim20] Lek-Heng Lim. Hodge laplacians on graphs. *Siam Review*, 62(3):685–715, 2020.
- [Llo96] Seth Lloyd. Universal quantum simulators. *Science*, 273(5278):1073–1078, 1996.
- [LMR13] Seth Lloyd, Masoud Mohseni, and Patrick Rebentrost. Quantum algorithms for supervised and unsupervised machine learning. *arXiv preprint arXiv:1307.0411*, 2013.
- [LSI⁺20] Seth Lloyd, Maria Schuld, Aroosa Ijaz, Josh Izaac, and Nathan Killoran. Quantum embeddings for machine learning. *arXiv preprint arXiv:2001.03622*, 2020.
- [Man80] Yuri Manin. Computable and uncomputable. *Sovetskoye Radio, Moscow*, 128:15, 1980.
- [MGB22] Sam McArdle, András Gilyén, and Mario Berta. A streamlined quantum algorithm for topological data analysis with exponentially fewer qubits. *arXiv preprint arXiv:2209.12887*, 2022.
- [MNKF18] Kosuke Mitarai, Makoto Negoro, Masahiro Kitagawa, and Keisuke Fujii. Quantum circuit learning. *Physical Review A*, 98(3):032309, 2018.
- [Nak18] Mikio Nakahara. *Geometry, topology and physics*. CRC press, 2018.
- [Ngh25] Nhat A Nghiem. Refined quantum algorithms for principal component analysis and solving linear system. *arXiv preprint arXiv:2504.00833*, 2025.
- [NGW23] Nhat A Nghiem, Xianfeng David Gu, and Tzu-Chieh Wei. Quantum algorithm for estimating betti numbers using a cohomology approach. *arXiv preprint arXiv:2309.10800*, 2023.
- [Ray24] Chaithanya Rayudu. Fermionic independent set and laplacian of an independence complex are qma-hard. *arXiv preprint arXiv:2411.03230*, 2024.
- [RBWL18] Patrick Rebentrost, Thomas R Bromley, Christian Weedbrook, and Seth Lloyd. Quantum hopfield neural network. *Physical Review A*, 98(4):042308, 2018.
- [RML14] Patrick Rebentrost, Masoud Mohseni, and Seth Lloyd. Quantum support vector machine for big data classification. *Physical Review Letters*, 113(13):130503, 2014.
- [Rud24] Dorian Rudolph. Towards a universal gateset for qma₁. *arXiv preprint arXiv:2411.02681*, 2024.
- [SBG⁺19] Maria Schuld, Ville Bergholm, Christian Gogolin, Josh Izaac, and Nathan Killoran. Evaluating analytic gradients on quantum hardware. *Physical Review A*, 99(3):032331, 2019.
- [SBSW20] Maria Schuld, Alex Bocharov, Krysta M Svore, and Nathan Wiebe. Circuit-centric quantum classifiers. *Physical Review A*, 101(3):032308, 2020.
- [Sch19] Maria Schuld. Machine learning in quantum spaces, 2019.

- [Sho99] Peter W Shor. Polynomial-time algorithms for prime factorization and discrete logarithms on a quantum computer. *SIAM Review*, 41(2):303–332, 1999.
- [SK19] Maria Schuld and Nathan Killoran. Quantum machine learning in feature hilbert spaces. *Physical Review Letters*, 122(4):040504, 2019.
- [SL23] Alexander Schmidhuber and Seth Lloyd. Complexity-theoretic limitations on quantum algorithms for topological data analysis. *PRX Quantum*, 4:040349, Dec 2023.
- [SP18] Maria Schuld and Francesco Petruccione. *Supervised learning with quantum computers*, volume 17. Springer, 2018.
- [SRZ⁺25] Alexander Schmidhuber, Michele Reilly, Paolo Zanardi, Seth Lloyd, and Aaron Lauda. A quantum algorithm for khovanov homology. *arXiv preprint arXiv:2501.12378*, 2025.
- [SSM21] Maria Schuld, Ryan Sweke, and Johannes Jakob Meyer. Effect of data encoding on the expressive power of variational quantum-machine-learning models. *Physical Review A*, 103:032430, Mar 2021.
- [SUK24a] Stefano Scali, Chukwudubem Umeano, and Oleksandr Kyriienko. Quantum topological data analysis via the estimation of the density of states. *Physical Review A*, 110(4):042616, 2024.
- [SUK24b] Stefano Scali, Chukwudubem Umeano, and Oleksandr Kyriienko. The topology of data hides in quantum thermal states. *APL Quantum*, 1(3), 2024.
- [UAS⁺21] Shashanka Ubaru, Ismail Yunus Akhalwaya, Mark S Squillante, Kenneth L Clarkson, and Lior Horesh. Quantum topological data analysis with linear depth and exponential speedup. *arXiv preprint arXiv:2108.02811*, 2021.
- [US16] Shashanka Ubaru and Yousef Saad. Fast methods for estimating the numerical rank of large matrices. In *International Conference on Machine Learning*, pages 468–477. PMLR, 2016.
- [USS17] Shashanka Ubaru, Yousef Saad, and Abd-Krim Seghouane. Fast estimation of approximate matrix ranks using spectral densities. *Neural Computation*, 29(5):1317–1351, 2017.
- [Was16] Larry Wasserman. Topological data analysis. *arXiv preprint arXiv:1609.08227*, 2016.
- [ZLY22] Xiao-Ming Zhang, Tongyang Li, and Xiao Yuan. Quantum state preparation with optimal circuit depth: Implementations and applications. *Physical Review Letters*, 129(23):230504, 2022.